Title: ***Neospora caninum*** **dense granule protein 7 regulates pathogenesis of neosporosis by modulating host immune response**

Short title: *Neospora* GRA7 contributes to parasite virulence

Authors: Yoshifumi Nishikawa[a]#, Naomi Shimoda[a], Ragab M. Fereig[a,b,c], Tomoya Moritaka[a], Kousuke Umeda[a], Maki Nishimura[a], Fumiaki Ihara[a], Kaoru Kobayashi[a], Yuu Himori[a], Yutaka Suzuki[d], Hidefumi Furuoka[e]

Author affiliations:

[a] National Research Center for Protozoan Diseases, Obihiro University of Agriculture and Veterinary Medicine, Inada-cho, Obihiro, Hokkaido 080-8555, Japan.

[b] Research Center for Global Agromedicine, Obihiro University of Agriculture and Veterinary Medicine, Obihiro, Hokkaido 080-8555, Japan.

[c] Department of Animal Medicine, Faculty of Veterinary Medicine, South Valley University, Qena City, Qena 83523, Egypt.

[d] Graduate School of Frontier Science, The University of Tokyo, Kashiwa, Chiba, Japan.

[e] Division of Pathobiological Science, Department of Basic Veterinary Medicine, Obihiro University of Agriculture and Veterinary Medicine, Obihiro 080-8555, Japan.

Corresponding author

E-mail: nisikawa@obihiro.ac.jp (YN)

ABSTRACT

Neospora caninum is a protozoan parasite closely related to *Toxoplasma gondii*. Neosporosis caused by *N. caninum* is considered one of the main causes of abortion in cattle and nervous-system dysfunction in dogs, and identification of the virulence factors of this parasite is important for the development of control measures. Here, we used a luciferase reporter assay to screen the dense granule proteins genes of *N. caninum*, and found that NcGRA6, NcGRA7, and NcGRA14 are involved in the activation of the NF-κB, calcium/calcineurin, and cAMP/PKA signals. To analyze the functions of these proteins and *Neospora* cyclophilin, we successfully knocked out their genes in the Nc1 strain using plasmids containing the CRISPR/Cas9 components. Among the deficient lines, the *NcGRA7*-deficient parasites showed reduced virulence in mice. An RNA sequencing analysis of infected macrophage cultures showed that NcGRA7 mainly regulates the host cytokine and chemokine production. The levels of IFN-γ in the ascites fluid, CXCL10 expression in the peritoneal cells, and CCL2 expression in the spleen were lower 5 days after infection with the *NcGRA7*-deficient parasite than after infection with the parental strain. The parasite burden and the degree of necrosis in the brains of mice infected with the *NcGRA7*-deficient parasite were also lower than in those of the parental strain. Collectively, our data suggest that both the NcGRA7-dependent activation of the inflammatory response and the parasite burden are important in *Neospora* virulence.

IMPORTANCE

Neospora caninum invades and replicates in a broad range of host species and cells within those hosts. The effector proteins exported by *Neospora* induce its pathogenesis by modulating the host immunity. We show that most of the transcriptomic effects in *N. caninum*-infected cells depend upon the activity of NcGRA7. A deficiency in NcGRA7 reduced the virulence of the parasite in mice. This study demonstrates the importance of NcGRA7 in the pathogenesis of neosporosis.

KEY WORDS:

Neospora caninum, NcGRA7, CRISPR/Cas9, macrophage, mouse

INTRODUCTION

Neospora caninum is a protozoan parasite belonging to the phylum Apicomplexa, and is closely related to *Toxoplasma gondii*. *Neospora caninum* infects a wide range of warm-blooded animals as intermediate hosts and dogs as the definitive host (1). Neosporosis is considered one of the main causes of abortion and neonatal mortality in cattle and nervous-system dysfunction in dogs (2,3). Importantly, bovine neosporosis entails significant economic losses (1,4,5). In humans, antibodies against *N. caninum* have been detected in Brazil, Korea, Northern Ireland, and the United States, although no viable parasite has been isolated from humans (4). With no effective drugs or vaccines available to control neosporosis (1), there is an urgent need to develop measures to control *N. caninum* infection. To develop new vaccines and drug targets for this disease, more scientific evidence of the molecular factors and genes involved in *Neospora* pathogenesis is required.

Neospora caninum primarily induces the host cellular immune response by invading and replicating in the host cells. Interferon γ (IFN-γ) plays an important role as the major mediator of resistance against *N. caninum* in vivo (6,7). In addition to IFN-γ-producing $CD4^+$ and $CD8^+$ T cells, different types of innate cells are required for the acquisition of protective immunity against *N. caninum* infection, including natural killer T cells, macrophages, and dendritic cells (8–11). The pathogenesis of *N. caninum* infection is closely associated with the host–parasite interaction, and the effector proteins exported by the parasite secretory organelles (rhoptries and dense granules) are key factors in its pathogenesis because they modulate the host immune response. Several proteins of *N. caninum* have been identified as effector molecules that could interact with host signaling pathways. The rhoptry proteins of *N. caninum*, NcROP5 and NcROP16, may be virulence factors because parasites deficient in these

proteins cause reduced mortality in mice (12,13). NcROP16 is also responsible for STAT3 activation (13). Similarly, the *Toxoplasma* rhoptry proteins, ROP5, ROP16, ROP18, and ROP38, contain protein kinase domains (14), and subvert and co-opt host-cell functions (15–17). Among other molecules of *N. caninum*, cyclophilin (NcCYP) appears to contribute to host cell migration (18) and profilin (NcPF) induces strong IFN-γ and interleukin 12 (IL-12) responses (19). Therefore, the effector proteins exported by *N. caninum* are key players in neosporosis.

In *T. gondii*, dense granule proteins also participate in the modulation of host cell functions. GRA6, GRA15, GRA16, and GRA24 are involved in the activation of the host transcription factor nuclear factor of activated T cells 4 (NFAT4), the activation of nuclear factor-kappa B (NF-κB), the regulation of host cell-cycle progression and the TP53 tumor suppressor signaling pathway, and the promotion of p38 mitogen-activated protein kinase activation, respectively (20–23). However, the dense granule proteins of *N. caninum* that directly activate cell signaling pathways in the host cells have not yet been identified. Therefore, we screened 18 potential dense granule proteins of *N. caninum* for their activation of host cell signaling pathways in this study. The *NcGRA6*, *NcGRA7*, or *NcGRA14* gene was knocked out in *N. caninum*, and we used the clustered regularly interspaced short palindromic repeats (CRISPR)-associated gene 9 (CRISPR/CAS9) system to examine the effects on the parasite phenotype. We demonstrate that NcGRA7 regulates the pathogenesis of neosporosis by modulating the host immune response.

RESULTS

Ectopic expression of *Neospora*-derived molecules robustly activates cell signaling pathways in 293T cells. Because *T. gondii* GRA proteins activate host cell

signaling pathways, we hypothesized that *N. caninum* GRA proteins, including NcCYP and NcPF, also manipulate host gene expression by activating signaling pathways in the host cells. We constructed mammalian expression vectors for 18 *N. caninum* GRA proteins, NcCYP, and NcPF, and assessed whether their expression, together with luciferase reporter plasmids carrying elements dependent on various transcription factors, activated the reporters (Fig. 1A). Among our target genes, *NcGRA6*, *NcGRA7*, and *NcGRA14* were involved in the activation of NF-κB signaling, calcium/calcineurin (NFAT) signaling, and cAMP/PKA (CRE) signaling (Fig. 1B).

Characterization of *NcGRA6*-, *NcGRA7*-, *NcGRA14*-, and *NcCYP*-deficient parasites in vitro and in vivo. To evaluate whether NcGRA6, NcGRA7, or NcGRA14 are involved in the virulence of *Neospora*, we generated gene-deficient parasites with the CRISPR/CAS9 system (Figs S1A–C, 2A). *NcCYP*-deficient parasites were also generated because it has been suggested that NcCYP induces IFN-γ production by peripheral blood mononuclear cells (24) and triggers the migration of murine and bovine cells (18) (Figs S1D, 2A). CRISPR plasmids targeting between nucleotide (nt) 86 and nt 87 in the *NcGRA6* gene, between nt 113 and nt 114 in the *NcGRA7* gene, between nt 110 and nt 111 in the *NcGRA14* gene, and between nt 753 and nt 754 in the *NcCYP* gene were constructed to allow the insertion of the pyrimethamine-resistance dihydrofolate reductase (DHFR*) cassette (Fig. S1). The CRISPR plasmids were then transferred into *N. caninum* strain Nc1 with electroporation, and the parasites were selected in the presence of pyrimethamine. To verify the successful establishment of the gene-deficient lines, PCR was used to confirm the insertion of the DHFR* cassette into the target gene in the clones obtained with limited dilution. The amplification of the target gene was negative and

the insertion of the DHFR* cassette into the target gene was confirmed in each deficient line (Fig. S1). The loss of the target genes was also confirmed with western blotting (Fig. 2A). Anti-NcGRA6 mouse serum detected a 33-kDa protein in the Nc1 strain, but not in the *NcGRA6*-deficient parasite. A rabbit NcGRA7 antibody detected three major proteins of 33, 26, and 18 kDa in the Nc1 strain, but not in the *NcGRA7*-deficient parasite. Anti-NcGRA14 mouse serum detected a 51-kDa protein in the Nc1 strain, but not in the N*cGRA14*-deficient parasite. A rabbit NcCYP antibody detected a 15-kDa protein in the Nc1 strain, but not in the *NcCYP*-deficient parasite. Additionally, we confirmed the loss of target protein expression by an immunofluorescent antibody test (IFAT), except in the case of the *NcGRA14*-deficient parasite (anti-NcGRA14 mouse serum did not specifically react with Nc1 by IFAT) (Figs. S2, S3).

We then assessed the physiological changes in the gene-deficient lines in vitro. The infection rates of the *NcGRA6*- (6.1 ± 3.3%) and *NcGRA7*-deficient lines (9.5 ± 3.2%) at 20 h postinfection in Vero cells were similar to those of the parental strain Nc1 (5.8 ± 1.1%) (Fig. 2B). The infection rates of the *NcGRA14*- (11.3 ± 1.3%) and *NcCYP*-deficient lines (16.6 ± 2.1%) at 20 h postinfection in Vero cells were significantly higher than those of the parental strain Nc1 ($P < 0.05$) (Fig. 2B). We measured the numbers of parasites in parasitophorous vacuoles (PV) at 48 h postinfection between strains (Fig. 2C). However, the deficient parasites displayed numbers of parasites per PV similar to the number in the parental strain Nc1 while reduced % at 16 parasites per PV was seen in *NcGRA6*-deficient line, suggesting that in vitro-proliferation rates were not affected by the loss of these proteins. Because *N. caninum* start to egress from host cells after 48 h postinfection in vitro, % egress of parasites at 72 h postinfection was measured (Fig. 2D). Among the gene-deficient

lines, *NcGRA7*-deficient line showed lower egress compared with the parental strain Nc1 ($P < 0.05$). The parasitic virulence of the lines was also compared in BLAB/c and C57BL/6 mice (Fig. 3A,B). Among the deficient lines, the *NcGRA7*-deficient line showed the lowest virulence relative to the parental strain Nc1 and the other deficient lines. The low virulence of the *NcGRA7*-deficient line was similar to that seen in Toll-like receptor 2 (TLR2)-deficient mice (Fig. 3C).

To confirm the loss of virulence in the *NcGRA7*-deficient line, a FLAG-tag-fused *NcGRA7* gene was introduced between nt 88 and nt 89 in the *Neospora* uracil phosphoribosyl transferase (*NcUPRT*) gene of the *NcGRA7*-deficient line with the CRISPR/CAS9 system (Fig. S3). The complemented parasites were selected in the presence of fluorouracil (5-FU). The PCR results showed the correct insertion of the FLAG-tag-fused *NcGRA7* gene into the *NcUPRT* gene. The expression of the FLAG-tag-fused NcGRA7 protein was confirmed with western blotting (Fig. 2A) and an IFAT (Fig. S3B). Three major proteins of 39, 34, and 25 kDa were detected in the *NcGRA7*-complemented parasite. The differences of molecular weights of NcGRA7 between the Nc1 strain and the *NcGRA7*-complemented parasite were 6-8 kDa. FLAG-tag has 22 amino acids (DYKDHDGDYKDHDIDYKDDDDK) and most amino acids in the tag are charged amino acids such as D, K and H (77%, 17/22). Charged amino acids may affect micelle formation between SDS and protein, resulting in different migration from expected size of protein on SDS-PAGE. Thus, the FLAG-tag-fused NcGRA7 proteins might be larger than the native NcGRA7 proteins because of the length and charge of amino acid in the FLAG-tag. We evaluated the band intensity between NcGRA7 in the Nc1 and the *NcGRA7*-complemented parasite by objective judgment using ImageJ software v. 1.49 (Mac version of NIH Image, http//rsb.info.nih.gov/nih-image/). The expression level of the

FLAG-tag-fused NcGRA7 protein in the *NcGRA7*-complemented parasite observed with western blotting was 19.2% of that in the Nc1, consistent with the results of RNA sequencing, shown in Table S1 (mean counts per million [CPM]: Nc1, 10,236.71; *NcGRA7*-deficient, 623.66; *NcGRA7*-complemented, 4,233.64). As shown in Fig. S3C, egress level of the *NcGRA7*-complemented parasite was similar to that of the Nc1. The virulence of the *NcGRA7*-complemented line in the infected BLAB/c mice was thus restored (Fig. 3D). The survival rate at 20 days postinfection of mice infected with *NcGRA7*-complemented parasite (7/8, 87.5%) was higher than that of mice infected with Nc1 (3/8, 37.5%) ($P = 0.04$), while the survival rates at 60 days postinfection were not significantly different between mice infected with Nc1 and *NcGRA7*-complemented parasite ($P = 0.52$).

Transcriptome and cytokine production of the *NcGRA7*-deficient parasite in macrophages. To understand the roles of NcGRA7, a transcriptomic sequencing analysis of infected macrophage cultures was performed (Fig. 4). The infection rates were similar among the parasite lines (Nc1: 4.9 ± 0.5%; *NcGRA7*-deficient parasite: 5.9 ± 0.8%; *NcGRA7*-complemented parasite: 5.3 ± 1.4%). We first examined the differentially expressed genes (DEGs) in the parasites and found that 15 genes, including nine genes encoding hypothetical proteins, were downregulated and four genes were upregulated in the *NcGRA7*-deficient parasite compared with their expression in the parental strain Nc1 (Table S1). Although these data demonstrated the *NcGRA7* deficiency, the complementation of the *NcGRA7* gene, and the expression of DHFR* in each parasite line, we could not confirm any clear changes in other *Neospora* genes based on the mean CPM values.

To analyze the pathways of host cells regulated by NcGRA7 in more detail, we analyzed the Kyoto Encyclopedia of Genes and Genomes (KEGG) pathways in which the host genes were involved (Table S2). Immune-response-related pathways, such as the IL-17 signaling pathway, the cytokine–cytokine receptor interaction pathway, and the tumor necrosis factor (TNF) signaling pathway were significantly enriched in the DEGs downregulated in macrophage cultures infected with the *NcGRA7*-deficient parasite compared with their expression in Nc1-infected cell cultures. Although only the Hippo signaling pathway was enriched in DEGs upregulated in macrophage cultures infected with the *NcGRA7*-deficient parasite, the false discovery rate (FDR) *p* value was 0.04. A heatmap of the gene expression associated with cytokine–cytokine receptor interactions showed that the expression levels of several cytokines and chemokines were changed as the expression levels of *NcGRA7* were altered in *N. caninum* (Fig. 4, Table S3). To identify the host genes regulated by NcGRA7, the DEGs up- or downregulated in macrophage cultures infected with the *NcGRA7*-deficient parasite were compared with the genes expressed in Nc1-infected cell cultures and ranked according to the degree of change in expression (Fig. 5, Table S4). When we considered the gene expression levels in macrophage cultures infected with the *NcGRA7*-complemented line, upregulated genes, such as *Cxcl3*, *Il1b*, *Serpinb*, *Slc6a9*, *Serpine1*, *Aldh1l2*, and *Siglece*, and downregulated genes, such as *Ccnd1*, *Rasgrp3*, *Uhrf1*, *Cavin1*, *Plau*, and *Cbr2*, were identified as NcGRA7-regulated genes (Table S4). The production of IL-12p40 and IL-6 in the macrophage cultures infected with the *NcGRA7*-deficient parasite was lower than in the Nc1-infected cell cultures, and the complementation of the *NcGRA7* gene in the *NcGRA7*-deficient line resulted in the partial restoration of cytokine production (Fig. 6). Together, these results indicate that NcGRA7 deficiency robustly

downregulated the immune-response-related pathways induced by *N. caninum* infection.

Measurement of inflammatory markers in vivo. Based on the results shown in Fig. 6, we measured the levels of IFN-γ, an inflammatory marker, in the ascites fluid of mice at 5 days postinfection (Fig. 7A). The IFN-γ levels were lower in the mice infected with the *NcGRA7*-deficient parasite than in mice infected with Nc1 or the *NcGRA7*-complemented line, indicating that NcGRA7 deficiency reduced the inflammatory response in vivo. To examine the effects of NcGRA7 deficiency on the inflammatory response at the tissue level, the mRNA expression of cytokines (TNF-α and IFN-γ), chemokines (CCL1, CCL2, CCL5, CCL7, CCL8, CCL17, CCL22, CXCL9, and CXCL10), chemokine receptors (CCR5, CCR7, CXCR3, and CXCR6), and inducible nitric oxide synthase in the peritoneal cells and spleens of mice was measured at 5 days postinfection. The expression of TNF-α, CCR5, CXCL9, and CXCL10 mRNAs was enhanced in the peritoneal cells by Nc1 infection, whereas the level of CXCL10 expression was lower in the peritoneal cells of mice infected with the *NcGRA7*-deficient parasite than in the Nc1-infected mice (Fig. 7B). The splenic expression of CCL2, CCL8, and CXCL9 was upregulated after *N. caninum* infection and *NcGRA7* deficiency reduced the expression levels of CCL2 to below those after Nc1 infection (Fig. 7C). The expression levels of CXCL10 in peritoneal cells and CCL2 in spleen were not significantly different between Nc1 and the *NcGRA7*-complemented line.

Parasite tissue burden. The number of parasites in the brain, lung, liver, and spleen tissues of mice were measured at 12 and 20 days postinfection with quantitative real-

time PCR (Fig. 8). Although no statistically significant difference was found between tissue samples from the same organs from the three groups at 12 days postinfection (Fig. 8A), the number of *NcGRA7*-deficient parasites was higher in the spleen, but lower in the brain than the number of Nc1 at 20 days postinfection (Fig. 8B).

Pathological analysis of infected mice. We performed a pathological analysis of the livers, spleens, lungs, and brains of the mice at 20 days postinfection. Scattered mild lymphocyte infiltration was observed in several livers and lungs, but no specific or differentiable lesions were found in the livers, spleens, or lungs of the mice infected with Nc1, the *NcGRA7*-deficient line, or the *NcGRA7*-complemented line. Brain lesions were common in infections with all lines, and consisted of scattered lymphocytic perivascular cuffing, meningitis, focal gliosis, and focal necrosis associated with lipid-laden macrophages and gliosis. However, the severity of infection, indicated by the number of necrotic lesions, varied across individuals and brain regions, and the number of necrotic lesions was lower in the brains of mice infected with the *NcGRA7*-deficient line than in those of the Nc1-infected mice (Fig. S4). Focal necrosis was mainly observed in the cerebrum and brain stem, and there was little in the cerebellum. In several cases, acidophilic tachyzoites were observed at the periphery of the necrotic lesions. In an immunohistochemical analysis, *N. caninum* antigen was detected in or around the inflammatory and necrotic lesions (Fig. 9). We confirmed the specificity of the reaction with rabbit NcGRA7 antibody using preimmune rabbit antibody and brain tissues of uninfected mouse (Fig. S4). The positive signal for NcGRA7 was observed as punctate or amorphous staining, in addition to *N. caninum* tachyzoites, in or around the lesions (Fig. 9C, D).

DISCUSSION

Gene deletion techniques and protein expression analyses are useful for studying the protein functions in parasites, to better understand parasite biology. The recent adaptation of the CRISPR/Cas9 technology has led to extremely efficient gene editing in apicomplexan parasites (e.g., *Plasmodium*, *Cryptosporidium* and *Toxoplasma*) (25). The CRISPR/Cas9 system was adapted to produce efficient targeted gene disruption and the site-specific insertions of selectable markers in *T. gondii* (26,27). Very recently, Arranz-Solís et al. (2018) reported that *Toxoplasma* CRISPR/Cas9 constructs successfully disrupted genes in an Nc-Spain7 isolate of *N. caninum* (28). Similarly, we used the universal pU6 plasmid (Addgene plasmid, pSAG1::CAS9-U6::sgUPRT), which contains Cas9 with a nuclear localization sequence driven by the *TgTUB1* promoter and a gRNA expression site driven by the *T. gondii* U6 promoter (27), to disrupt and insert genes into the Nc1 strain of *N. caninum*, and confirm that the *Toxoplasma* CRISPR/Cas9 constructs were successfully used in the present study.

Three North American clonal lineages of *T. gondii* (types I, II, and III) differ in their activation of the immune responses, including the host NF-κB pathway. The type II strains induce a high level of NF-κB p65 translocation, whereas the types I and III strains do not (21). Although the dense granule proteins, including GRA6, GRA15, GRA16, and GRA24, are important virulence factors in *T. gondii* (20–23), some dense granule proteins show type-specific functions. Ma et al. (2014) reported that according to a luciferase reporter assay, which was similar to the system we used in this study, the transfection of 293T cells with the cDNA of *Toxoplasma* GRA6 (type I strain) or GRA15 (type II strain) activated NF-κB or NFAT signal, respectively (20). Furthermore, *Toxoplasma* GRA14 (type II strain) also activated the NF-κB signal, although at an activity level lower than that induced by GRA15 (20). Interestingly,

311 there is no homologue of *Toxoplasma* GRA15 in the *Neospora* genome (from the
312 Toxoplasma Genomics Resource, ToxoDB). In our luciferase reporter assay, several
313 dense granule proteins of *N. caninum* (NcGRA6, NcGRA7, and NcGRA14) activated
314 the NF-κB, NFAT, and cAMP/PKA signals. These results suggest that the dense
315 granule proteins of *N. caninum* contribute to the activation of the host immune
316 responses.

317 In this study, we generated *NcGRA6*-, *NcGRA7*-, *NcGRA14*-, and *NcCYP*-deficient
318 *N. caninum* to examine the roles of the encoded proteins. Among these constructs, the
319 *NcGRA7*-deficient parasite showed reduced virulence in immunocompetent mice and
320 immunocompromised (TLR2-deficient) mice, whereas there was no significant
321 difference in the infection rate or intracellular growth of the parental strain Nc1 and
322 the *NcGRA7*-deficient strain in vitro. Interestingly, egress of the *NcGRA7*-deficient
323 line delayed compared with that of the Nc1. It may reduce the parasite burden in host
324 body in vivo. The infection rates of the *NcGRA14*- and *NcCYP*-deficient lines were
325 higher than that of Nc1. So we must understand these phenotypes in future study. A
326 recent study showed that the loss of NcROP5 by *N. caninum* led to a reduction in
327 mouse mortality and reduced *NcGRA7* transcription in the parasite (12). According to
328 ToxoDB, sequences that share high identity with TgROP5 (TgROP5A, TgROP5B,
329 and TgROP5C) have been detected the genome of the *N. caninum* Liverpool strain:
330 NcLIV_060730, NcLIV_060740, and NcLIV_060741, respectively (12, 29). On the
331 contrary, RNA sequencing in this study showed no significant differences in the
332 expression levels of *Neospora* ROP5 in Nc1 and the *NcGRA7*-deficient and *NcGRA7*-
333 complemented lines (Table S1). Moreover, the cerebral loads of the parasite in mice
334 infected with the *NcROP16*-deficient strain were significantly lower than the loads in
335 mice infected with the Nc1 strain (13), but the expression levels of NcROP16

(NcLIV_025120) did not differ in the parasite lines in our study (Table S1). Excluding inserted and deficient genes, we found that 14 genes were downregulated or upregulated in the *NcGRA7*-deficient parasite, including nine genes encoding hypothetical proteins and three genes encoding unknown proteins. These genes might be related to metabolic enzymes, transporters, or cell-surface antigens that are altered in response to NcGRA7 deficiency. Therefore, NcGRA7 is a key molecule in the virulence of *N. caninum* in mice. Although it is unknown whether NcGRA7 interacts with host factors or other parasite molecules, *Toxoplasma* GRA7 increases the turnover of immunity-related GTPases and contributes to the parasite's acute virulence in the mouse (30). We identified several host macrophage genes as 'core' NcGRA7-regulated genes in this study. Our results suggest that NcGRA7 may be a master regulator to control host immune response. Because the secretion of NcGRA7 into the host-cell cytosol was observed in Nc1-infected Vero cells 48 h postinfection (Figs. S2A, S6), NcGRA7 may interact with host protein(s) involved in the host immune response. Therefore, in a future study, we will identify the NcGRA7-binding protein(s) to further clarify the function of NcGRA7.

In a KEGG pathway analysis of *N. caninum*-infected macrophage cultures, we demonstrated that NcGRA7 robustly activates the host signaling pathways, especially the production of cytokines and chemokines, as shown in Table S3. In macrophages, the production of the inflammatory cytokines IL-12p40 and IL-6 is regulated by NcGRA7. The levels of IFN-γ (an inflammatory marker) were also lower in the ascites fluid of mice infected with the *NcGRA7*-deficient parasites than in that of mice infected with Nc1 or the *NcGRA7*-complemented parasite. These results support the notion of NcGRA7-dependent inflammatory responses. The expression data for DEGs also showed that chemokine (C-X-C motif) ligand 3 (CXCL3) was upregulated in an

NcGRA7-dependent manner in macrophages in vitro. The expression levels of CXCL10 in the peritoneal cells and of CCL2 in the spleen were higher in the mice infected with the parental strain of *N. caninum* than in those infected with the *NcGRA7*-deficient parasite. CCL2, CXCL3, and CXCL10 control the migration and adhesion of immune cells by interacting with the cell-surface chemokine receptors CCR2/4, CXCR2, and CXCR3, respectively (31–33). Therefore, NcGRA7 may play a role in parasite migration within the host body because infected dendritic cells facilitate the systemic dissemination of *N. caninum* in mice (34). In the present study, the dissemination of the *NcGRA7*-deficient parasite to the brain was lower than that of the parental strain Nc1, suggesting that the regulation of chemokines by NcGRA7 affects the parasite burden.

We also defined several host macrophage genes as 'core' NcGRA7-regulated genes, as shown in Table S4. The upregulation of gene *Serpinb2* and *Serpine1* and the downregulation of *Plau* confirmed them as NcGRA7-regulated genes. Plasminogen activator inhibitor 1 (PAI-1), encoded by *Serpine1*, and plasminogen activator inhibitor 2 (PAI-2), encoded by *Serpinb2*, are serine protease inhibitors (serpins) that function as the principal inhibitors of the tissue plasminogen activator and urokinase encoded by *Plau*. Elevated PAI-1 is a risk factor for thrombosis and atherosclerosis (35). PAI-2 is only present in detectable quantities in the blood during pregnancy because it is produced by the placenta (36). Although the effects of PAI-1 and PAI-2 on *N. caninum* infection are unknown, they may be associated with the pathogenesis of peripheral and placental infections. The expression of *Slc6a9*, encoding sodium- and chloride-dependent glycine transporter 1, was also upregulated by NcGRA7. This transporter may play a role in the regulation of glycine levels in *N*-methyl-D-aspartate-receptor-mediated neurotransmission (37). In our previous study, we showed that the

386 expression of *Slc6a5*, which encodes sodium- and chloride-dependent glycine
387 transporter 2, was lower in symptomatic mice than in asymptomatic mice (38). Mice
388 deficient in glycine transporter 2 also showed neuromotor abnormalities, such as
389 spasticity, hind feet clasping, and tremor (39). Therefore, an imbalance in glycine
390 levels in the brain may be involved in the neuronal symptoms of *N. caninum* infection.
391 Although *Aldh1l2*, encoding mitochondrial 10-formyltetrahydrofolate dehydrogenase,
392 and *Siglece*, encoding sialic acid-binding Ig-like lectin 12, were identified as
393 NcGRA7-regulated genes, the contributions of these genes to *N. caninum* infection
394 are not known. Our pathological analysis indicated that NcGRA7 deficiency reduced
395 the number of necrotic lesions in the brain. NcGRA7 may associated with the tissue
396 damage that follows the inflammatory response, such as the migration of
397 inflammatory cells and the production of inflammatory cytokines, increasing the
398 virulence in the central nervous system.

399 Several host genes were downregulated by NcGRA7 in macrophages (Table S4).
400 *Ccnd1* (encoding G1/S-specific cyclin D1), *Uhrf1* (ubiquitin-like, containing PHD
401 and RING finger domains, 1), and *Rasgrp3* (RAS, guanyl releasing protein 3) encode
402 proteins that regulate the cell cycle and RAS signaling (40–42). *Toxoplasma* infection,
403 but not *Neospora* infection, induces an increase in the levels of c-MYC, a tightly
404 regulated transcription factor involved in vital cellular processes, including cell-cycle
405 progression, apoptosis, cell differentiation, and metabolism (43, 44). Therefore, the
406 roles of these genes in *N. caninum* infection should be examined carefully in future
407 studies. Interestingly, the lipid-metabolism-related genes *Cavin1* (caveolae associated
408 protein 1) and *Cbr2* (carbonyl reductase 2) were also identified as NcGRA7-
409 downregulated genes, which means that the parental strain of *N. caninum* inhibits the
410 expression of these genes. *Cavin1* is crucial for caveola formation and function (45).

411 Caveolae have several functions in signal transduction and are also believed to play
412 roles in mechanoprotection, mechanosensation, endocytosis, oncogenesis, and the
413 uptake of pathogens (46). The expression of *Cbr2* (encoding AP27) is linked to
414 adipogenic differentiation (47). However, it is unknown whether *N. caninum* inhibits
415 caveola formation or adipogenic differentiation.

416 The expression level of NcGRA7 in *NcGRA7*-complemented parasites was about
417 37.6% as mRNA level and 19.2% as protein level of that in the parental strain Nc1.
418 This difference may be due to promotor activity because the *Toxoplasma* GRA1
419 promotor was used in the complemented parasite. Although survival rates at 60 days
420 postinfection were not significantly different between mice infected with Nc1 and
421 *NcGRA7*-complemented parasites ($P = 0.52$), the survival rate of mice infected with
422 the *NcGRA7*-complemented parasite (7/8, 87.5%) at 20 days postinfection was higher
423 than that of Nc1-infected mice (3/8, 37.5%) ($P = 0.04$). This result suggests that the
424 expression level of NcGRA7 may affect acute virulence of the parasite. The
425 transcriptome of infected macrophage cultures showed broad changes of gene
426 expression related to immune response-related pathways in a NcGRA7-dependent
427 manner. When considering the gene expression levels in macrophage cultures infected
428 with the *NcGRA7*-complemented line, upregulated genes, such as *Cxcl3*, *Il1b*, *Serpinb*,
429 *Slc6a9*, *Serpine1*, *Aldh1l2*, and *Siglece*, and downregulated genes, such as *Ccnd1*,
430 *Rasgrp3*, *Uhrf1*, *Cavin1*, *Plau*, and *Cbr2*, were identified as highly sensitive genes
431 regulated by NcGRA7. The production of IL-12p40 and IL-6 in the macrophage
432 cultures infected with *NcGRA7*-deficient parasites significantly decreased compared
433 with Nc1-infected cell cultures. However, the cytokine levels of the macrophage
434 cultures infected with *NcGRA7*-complemented parasite did not reach the levels in
435 Nc1-infected cell cultures. In addition, compared with Nc1 infection, levels of IFN-γ

436 in ascites fluid, CXCL10 mRNA expression in peritoneal cells and CCL2 mRNA
437 expression in spleen were decreased in mice at 5 days after infection with *NcGRA7*-
438 deficient parasites, but these levels were partially recovered on infection with
439 *NcGRA7*-complemented parasites. These results may be associated with the parasite
440 burdens in spleen and brain at 20 days postinfection. Because chemokines and
441 chemokine receptors play a crucial role in the migration of parasite-infected immune
442 cells into several organs, the expression levels of NcGRA7 will affect the parasite
443 burden. Thus, suitable levels of NcGRA7 expression will be required for the
444 phenotype of parental strain Nc1, such as its virulence and gene expression profiles in
445 both the host and parasite.

446 Previous studies have demonstrated the antigenicity of NcGRA7 as a potential
447 vaccine antigen (48), but its function has not been determined. In the present study,
448 we show that NcGRA7 is a virulence factor in *N. caninum* infection. Although
449 nervous-system dysfunction and abortion are very important clinical symptoms of
450 neosporosis, the molecular mechanism of disease onset is largely unknown. Our
451 research approach, screening for potential virulence factors in *N. caninum*, provides
452 valuable scientific information and extends our understanding of neosporosis. We
453 identified several NcGRA7-regulated host genes with a comprehensive transcriptome
454 analysis. However, further research is required to clarify the association between
455 NcGRA7 and the host genes it regulates and their effects on the neurological
456 symptoms and abortion associated with neosporosis.

457

458 **MATERIALS AND METHODS**

459 **Ethics statement.** This study was performed in strict accordance with the
460 recommendations of the Guide for the Care and Use of Laboratory Animals of the

461 Ministry of Education, Culture, Sports, Science and Technology, Japan. The protocol
462 was approved by the Committee on the Ethics of Animal Experiments at Obihiro
463 University of Agriculture and Veterinary Medicine, Obihiro, Japan (permit numbers
464 24-16, 29-42, 28-47). All surgery was performed under isoflurane anesthesia and
465 every effort was made to minimize animal suffering.
466
467 **Animals.** C57BL/6 and BALB/c mice, 6–8 weeks of age, were obtained from Clea
468 Japan (Tokyo, Japan). Homozygous *TLR2*-knockout (*Tlr2*$^{-/-}$) mice were a kind gift
469 from Dr. Satoshi Uematsu and Dr. Shizuo Akira (Osaka University, Osaka, Japan)
470 (49). The animals were housed under specific-pathogen-free conditions in the animal
471 facility of the National Research Center for Protozoan Diseases at Obihiro University
472 of Agriculture and Veterinary Medicine, Obihiro, Japan. The animals used in this
473 study were treated and used according to the Guiding Principles for the Care and Use
474 of Research Animals published by the Obihiro University of Agriculture and
475 Veterinary Medicine.
476
477 **Parasite and cell cultures.** *Neospora caninum* (Nc1 strain) was maintained in African
478 green monkey kidney epithelial cells (Vero cells) cultured in Eagle's minimum
479 essential medium (EMEM; Sigma, St. Louis, MO, USA) supplemented with 8% heat-
480 inactivated fetal bovine serum (FBS). Human embryonic kidney cells (293T cells) and
481 the peritoneal macrophages were cultured in Dulbecco's modified Eagle's medium
482 (Sigma) supplemented with 10% heat-inactivated FBS. For the purification of
483 tachyzoites, parasites and host-cell debris were washed with cold phosphate-buffered
484 saline (PBS), and the final pellet was resuspended in cold PBS and passed through a
485 27-gauge needle and a 5.0 μm-pore filter (Millipore, Bedford, MA, USA).

Plasmid construction. All the plasmids and primers used in this study are listed in Tables S5 and S6 in the Supplemental Material. Further details of the plasmid construction can be found in the Supplemental Methods in the Supplemental Material.

Luciferase assay. 293T cells were transiently transfected with the reporter plasmid for the luciferase assay (Table 1) together with the pGL4.74 control *Renilla* luciferase expression vector (Promega) and the mammalian expression plasmid of *Neospora* genes, with FuGENE® HD Transfection Reagent (Promega), according to the manufacturer's instructions. At 20 h posttransfection, the luciferase activities in the total cell lysates were measured with the Dual-Glo® Luciferase Assay System (Promega).

Generation of *NcGRA6*-, *NcGRA7*-, *NcGRA14*-, and *NcCYP*-knockout lines. To disrupt the *NcGRA6*, *NcGRA7*, *NcGRA14*, and *NcCYP* genes in Nc1, we cotransfected the parasite with 50 μg of each CRISPR plasmid (pSAG1::CAS9-U6::sgNcGRA6, pSAG1::CAS9-U6::sgNcGRA7 pSAG1::CAS9-U6::sgNcGRA14, or pSAG1::CAS9-U6::sgNcCyp), together with an amplicon containing the homologous regions surrounding the pyrimethamine-resistance (DHFR*) cassette (5 μg), prepared by PCR amplification using the primers listed in Table 2. The electroporation of tachyzoites was performed as described previously (50). Stably resistant clones were selected by growth in pyrimethamine (1 μM) for 10–14 days and were subsequently screened with PCR to ensure the correct integration of DHFR* into each target gene locus (see

Fig. S1, Table 2). The PCR-positive clones were further analyzed with western blotting to confirm the loss of the target gene.

Generation of *NcGRA7*-complemented line. To complement the *NcGRA7* gene, we transfected the *NcGRA7*-deficient parasite with pSAG1::CAS9-U6::sgNcUPRT (50 μg) and the *NcGRA7*–FLAG DNA fragment (5 μg) containing the *Toxoplasma* GRA1 5′-UTR and GRA2 3′-UTR, prepared with PCR amplification from pDMG-NcGRA7FLAG and the primers listed in Table 2. Stably resistant clones were selected by growth on fluorouracil (10 μM) for 8 days and were subsequently screened with PCR to ensure the correct integration of *NcGRA7*–FLAG into the *Neospora UPRT* gene locus (see Fig. S3A). PCR-positive clones were further analyzed with western blotting and IFAT to confirm the expression of the NcGRA7–FLAG protein (Figs 2A and S3B).

***Neospora caninum* infection in mice.** To compare the parasites' virulence in mice, BALB/c, C57BL/6J, and *Tlr2*$^{-/-}$ mice were intraperitoneally inoculated with *N. caninum* (1×10^6 tachyzoites/mouse). The mice were observed daily for up to 60 days postinfection. The parasite burdens were quantified in the brains, lungs, livers, and spleens of the BALB/c mice at 5 and 12 days postinfection. To analyze mRNA expression, spleen and peritoneal exudate cells were collected from the BALB/c mice at 5 days postinfection. For the pathological analysis and immunohistochemistry, brain, lung, liver, and spleen tissues were collected from the BALB/c mice at 20 and 30 days postinfection, respectively.

Monolayer cultures of peritoneal macrophages. Mouse peritoneal macrophages were collected from mice 4 days after the intraperitoneal injection of 1 ml of 4.05% brewer-modified BBL™ thioglycolate medium (Becton and Dickinson, Sparks, MD, USA) by washing their peritonea with 5 ml of cold PBS. After harvesting, the cells were centrifuged at 800 × *g* for 10 min and suspended in Dulbecco's modified Eagle's medium (DMEM) supplemented with 10% FBS. A macrophage suspension (2×10^6 cells per well) was added to 12-well tissue culture microplates. The suspension was incubated at 37°C for 3 h, washed thoroughly to remove nonadherent cells, and incubated further at 37°C overnight. Then 2×10^5 parasites were added to each well. At 2 h postinfection, the extracellular parasites were washed away and DMEM supplemented with 10% FBS was added. At 20 h postinfection, the culture supernatants and cells were collected for the measurement of cytokines and RNA extraction, respectively.

RNA sequencing. RNA from the macrophage cultures was sequenced as described in our previous studies (38,51,52). Briefly, 1 μg of total RNA was subjected to polyA selection and a sequence library was constructed with the TruSeq RNA Sample Prep Kit (Illumina, San Diego, CA, USA). The library generated was sequenced with 36-bp single-end reads using the Illumina Genome Analyzer IIx and TruSeq SBS Kit v5-GA (36-cycle) (Illumina), according to the manufacturer's instructions. Raw sequence reads were subjected to quality control, and the cleaned reads were mapped to the reference mouse genome (mm10) with CLC Genomics Workbench version 10 (GWB; CLC bio, Aarhus, Denmark) (read mapping parameters: minimum fraction length of read overlap = 0.95, minimum sequence similarity = 0.95). The remaining unmapped reads were mapped to the reference *N. caninum* Liverpool strain genome (ToxoDB-

35_NcaninumLIV) (read mapping parameters: minimum fraction length of read overlap = 0.8, minimum sequence similarity = 0.8). Only uniquely mapped reads were retained for further analysis. All the samples were subjected to principal component analysis (PCA) using the PCA for RNAseq function in CLC GWB, to gain an overview of the whole expression data and look for classification patterns.

Identification of DEGs. For both the host and parasite gene expression data, the expression of each gene was compared between the Nc1 and *NcGRA7*-deficient parasites using the Differential Expression for RNA-seq function in CLC GWB. DEGs were identified as genes with a log2-fold change of > 1 or < -1 and FDR < 0.05.

KEGG pathway enrichment analysis. The KEGG database is a bioinformatic tool that assembles large-scale molecular datasets, such as gene lists, into biological pathway maps (53). The list of host DEGs was subjected to a KEGG pathway enrichment analysis using the clusterProfiler package (54) in the statistical environment R to assess their overarching function. Following CPM normalization, the expression of each gene in the enriched pathways was normalized with Z-score normalization and visualized. Normalized gene expression was visualized in a heatmap using the heatmap.2 function (55) in the gplots package in R. The genes were hierarchically clustered based on the Pearson correlation distance and the group average method.

Cytokine enzyme-linked immunosorbent assays (ELISAs). The supernatants of macrophage cultures and the ascites fluids of mice were collected to measure the IL-6,

583 IL-12p40, and IFN-γ levels with ELISA kits (Mouse OptEIA ELISA Set, BD
584 Biosciences, San Jose, CA, USA), according to the manufacturer's instructions. The
585 cytokine concentrations were calculated from curves generated from cytokine
586 standards analyzed on the same plates.

587

588 **Real-time reverse transcription (RT)–PCR analysis of chemokine expression.**
589 Total RNA was extracted from cells or homogenized tissues using TRI Reagent®
590 (Sigma-Aldrich). The RNA was reverse transcribed with the PrimeScript™ II 1st
591 strand cDNA Synthesis Kit (Takara Bio Inc., Shiga, Japan), following the
592 manufacturer's instructions. The cDNA was amplified with RT–PCR using
593 PowerUp™ SYBR® Green Master Mix (Thermo Fisher Scientific Inc., MA, USA)
594 and 500 nM gene-specific primers in a 10 µl total reaction volume, according to the
595 manufacturer's protocol. The primer sequences used for real-time RT–PCR are shown
596 in Table 2. *Actb* (encoding β-actin) was selected as the internal control gene using
597 RefFinder (56). The relative mRNA levels were calculated as described previously
598 (10).

599

600 **DNA isolation and real-time PCR analysis of *N. caninum* distribution.** DNA was
601 extracted from the tissues (brain, liver, lungs, and spleen) as follows. Each tissue or
602 organ was thawed in 10 volumes of extraction buffer (0.1 M Tris-HCl [pH 9.0], 1%
603 SDS, 0.1 M NaCl, 1 mM EDTA) and 100 µg/ml proteinase K at 55 °C. The DNA
604 was purified with phenol–chloroform extraction and ethanol precipitation. The
605 parasite DNA was then amplified with primers specific to the *N. caninum Nc5* gene
606 (Table 2). Amplification, data acquisition, and data analysis were performed in the

ABI Prism 7900HT Sequence Detection System (Applied Biosystems), and the cycle threshold values (Ct) were calculated as described previously (10,38). A standard curve was constructed using tenfold serial dilutions of *N. caninum* DNA extracted from 1×10^5 parasites; thus, the curve ranged from 0.01 to 10,000 parasites. Parasite number was calculated from the standard curve.

Statistical analysis. Data are expressed as means ± standard deviations or as scatter diagrams. The various assay conditions were evaluated with analysis of variance (ANOVA) followed by Tukey's multiple-comparisons test. The significance of the differences in survival at 60 days postinfection was analyzed with a χ^2 test. A *P*-value < 0.05 was considered statistically significant.

Funding

This research was supported by a Grant-in-Aid for Scientific Research (B) from the Ministry of Education, Culture, Sports, Science and Technology of Japan KAKENHI (15H04589, 18H02335).

ACKNOWLEDGMENTS

We thank Dr. Dubey (United States Department of Agriculture, Agriculture Research Service, Livestock and Poultry Sciences Institute, Parasite Biology and Epidemiology Laboratory, MD, USA) for the *N. caninum* Nc1 isolate. We also thank the Center for Omics and Bioinformatics, Graduate School of Frontier Sciences, the University of Tokyo, for determining the nucleotide sequences and their analysis. We thank Janine Miller, PhD, from Edanz Group (www.edanzediting.com/ac) for editing a draft of this manuscript.

632

633 **REFERENCES**

634 1. Dubey JP, Schares G. 2011. Neosporosis in animals--the last five years. Vet
635 Parasitol 180:90–108.
636 2. Hall CA, Reichel MP, Ellis JT. 2005. Neospora abortions in dairy cattle: diagnosis,
637 mode of transmission and control. Vet Parasitol 128:231–241.
638 3. Lyon C. 2010. Update on the diagnosis and management of Neospora caninum
639 infections in dogs. Top Companion Anim Med 25:170–175.
640 4. Dubey JP, Schares G, Ortega-Mora LM. 2007. Epidemiology and control of
641 neosporosis and Neospora caninum. Clin Microbiol Rev 20:323–367.
642 5. Reichel MP, Alejandra Ayanegui-Alcérreca M, Gondim LFP, Ellis JT. 2013. What
643 is the global economic impact of Neospora caninum in cattle - the billion dollar
644 question. Int J Parasitol 43:133–142.
645 6. Baszler TV, Long MT, McElwain TF, Mathison BA. 1999. Interferon-gamma and
646 interleukin-12 mediate protection to acute Neospora caninum infection in BALB/c
647 mice. Int J Parasitol 29:1635–1646.
648 7. Nishikawa Y, Tragoolpua K, Inoue N, Makala L, Nagasawa H, Otsuka H, Mikami
649 T. 2001. In the absence of endogenous gamma interferon, mice acutely infected
650 with Neospora caninum succumb to a lethal immune response characterized by
651 inactivation of peritoneal macrophages. Clin Diagn Lab Immunol 8:811–816.
652 8. Nishikawa Y, Zhang H, Ibrahim HM, Yamada K, Nagasawa H, Xuan X. 2010.
653 Roles of CD122+ cells in resistance against Neospora caninum infection in a
654 murine model. J Vet Med Sci 72:1275–1282.
655 9. Abe C, Tanaka S, Ihara F, Nishikawa Y. 2014. Macrophage depletion prior to
656 Neospora caninum infection results in severe neosporosis in mice. Clin Vaccine
657 Immunol. 21:1185–1188.

10. Abe C, Tanaka S, Nishimura M, Ihara F, Xuan X, Nishikawa Y. 2015. Role of the chemokine receptor CCR5-dependent host defense system in Neospora caninum infections. Parasit Vectors 8:5.

11. Teixeira L, Botelho AS, Mesquita SD, Correia A, Cerca F, Costa R, Sampaio P, Castro AG, Vilanova M. 2010. Plasmacytoid and conventional dendritic cells are early producers of IL-12 in Neospora caninum-infected mice. Immunol Cell Biol 88:79–86.

12. Ma L, Liu J, Li M, Fu Y, Zhang X, Liu Q. 2017. Rhoptry protein 5 (ROP5) Is a Key Virulence Factor in Neospora caninum. Front Microbiol 8:370.

13. Ma L, Liu G, Liu J, Li M, Zhang H, Tang D, Liu Q. 2017. Neospora caninum ROP16 play an important role in the pathogenicity by phosphorylating host cell STAT3. Vet Parasitol 243:135–147.

14. Peixoto L, Chen F, Harb OS, Davis PH, Beiting DP, Brownback CS, Ouloguem D, Roos DS. 2010. Integrative genomic approaches highlight a family of parasite-specific kinases that regulate host responses. Cell Host Microbe 8:208–218.

15. Dubremetz JF. 2007. Rhoptries are major players in Toxoplasma gondii invasion and host cell interaction. Cell Microbiol 9:841–848.

16. Hunter CA, Sibley LD. 2012. Modulation of innate immunity by Toxoplasma gondii virulence effectors. Nat Rev Microbiol 10:766–778.

17. Kemp LE, Yamamoto M, Soldati-Favre D. 2013. Subversion of host cellular functions by the apicomplexan parasites. FEMS Microbiol Rev 37:607–631.

18. Kameyama K, Nishimura M, Punsantsogvoo M, Ibrahim HM, Xuan X, Furuoka H, Nishikawa Y. 2012. Immunological characterization of Neospora caninum cyclophilin. Parasitology 139:294–301.

683 19. Jenkins MC, Tuo W, Feng X, Cao L, Murphy C, Fetterer R. 2010. Neospora
684 caninum: cloning and expression of a gene coding for cytokine-inducing profilin.
685 Exp Parasitol 125:357–362.
686 20. Ma JS, Sasai M, Ohshima J, Lee Y, Bando H, Takeda K, Yamamoto M. 2014.
687 Selective and strain-specific NFAT4 activation by the Toxoplasma gondii
688 polymorphic dense granule protein GRA6. J Exp Med 211:2013–2032.
689 21. Rosowski EE, Lu D, Julien L, Rodda L, Gaiser RA, Jensen KDC, Saeij JPJ.
690 2011. Strain-specific activation of the NF-kappaB pathway by GRA15, a novel
691 Toxoplasma gondii dense granule protein. J Exp Med 208:195–212.
692 22. Bougdour A, Durandau E, Brenier-Pinchart M-P, Ortet P, Barakat M, Kieffer
693 S, Curt-Varesano A, Curt-Bertini R-L, Bastien O, Coute Y, Pelloux H, Hakimi M-
694 A. 2013. Host cell subversion by Toxoplasma GRA16, an exported dense granule
695 protein that targets the host cell nucleus and alters gene expression. Cell Host
696 Microbe 13:489–500.
697 23. Braun L, Brenier-Pinchart M-P, Yogavel M, Curt-Varesano A, Curt-Bertini R-
698 L, Hussain T, Kieffer-Jaquinod S, Coute Y, Pelloux H, Tardieux I, Sharma A,
699 Belrhali H, Bougdour A, Hakimi M-A. 2013. A Toxoplasma dense granule protein,
700 GRA24, modulates the early immune response to infection by promoting a direct
701 and sustained host p38 MAPK activation. J Exp Med 210:2071–2086.
702 24. Tuo W, Fetterer R, Jenkins M, Dubey JP. 2005. Identification and
703 characterization of Neospora caninum cyclophilin that elicits gamma interferon
704 production. Infect Immun 73:5093–5100.
705 25. Suarez CE, Bishop RP, Alzan HF, Poole WA, Cooke BM. 2017. Advances in
706 the application of genetic manipulation methods to apicomplexan parasites. Int J
707 Parasitol 47:701–710.

708 26. Shen B, Brown KM, Lee TD, Sibley LD. 2014. Efficient gene disruption in
709 diverse strains of Toxoplasma gondii using CRISPR/CAS9. MBio 5:e01114-01114.
710 27. Sidik SM, Hackett CG, Tran F, Westwood NJ, Lourido S. 2014. Efficient
711 genome engineering of Toxoplasma gondii using CRISPR/Cas9. PLoS ONE
712 9:e100450.
713 28. Arranz-Solís D, Regidor-Cerrillo J, Lourido S, Ortega-Mora LM, Saeij JPJ.
714 2018. Toxoplasma CRISPR/Cas9 constructs are functional for gene disruption in
715 Neospora caninum. Int J Parasitol. In press.
716 29. Behnke MS, Khan A, Wootton JC, Dubey JP, Tang K, Sibley LD. 2011.
717 Virulence differences in Toxoplasma mediated by amplification of a family of
718 polymorphic pseudokinases. Proc Natl Acad Sci USA 108:9631–9636.
719 30. Alaganan A, Fentress SJ, Tang K, Wang Q, Sibley LD. 2014. Toxoplasma
720 GRA7 effector increases turnover of immunity-related GTPases and contributes to
721 acute virulence in the mouse. Proc Natl Acad Sci USA 111:1126–1131.
722 31. Craig MJ, Loberg RD. 2006. CCL2 (Monocyte Chemoattractant Protein-1) in
723 cancer bone metastases. Cancer Metastasis Rev 25:611–619.
724 32. Smith DF, Galkina E, Ley K, Huo Y. 2005. GRO family chemokines are
725 specialized for monocyte arrest from flow. Am J Physiol Heart Circ Physiol
726 289:H1976-1984.
727 33. Dufour JH, Dziejman M, Liu MT, Leung JH, Lane TE, Luster AD. 2002. IFN-
728 gamma-inducible protein 10 (IP-10; CXCL10)-deficient mice reveal a role for IP-
729 10 in effector T cell generation and trafficking. J Immunol 168:3195–3204.
730 34. Collantes-Fernandez E, Arrighi RBG, Alvarez-García G, Weidner JM,
731 Regidor-Cerrillo J, Boothroyd JC, Ortega-Mora LM, Barragan A. 2012. Infected

732 dendritic cells facilitate systemic dissemination and transplacental passage of the
733 obligate intracellular parasite Neospora caninum in mice. PLoS ONE 7:e32123.
734 35. Vaughan DE. 2005. PAI-1 and atherothrombosis. J Thromb Haemost 3:1879–
735 1883.
736 36. Astedt B, Lindoff C, Lecander I. 1998. Significance of the plasminogen
737 activator inhibitor of placental type (PAI-2) in pregnancy. Semin Thromb Hemost
738 24:431–435.
739 37. Kim KM, Kingsmore SF, Han H, Yang-Feng TL, Godinot N, Seldin MF,
740 Caron MG, Giros B. 1994. Cloning of the human glycine transporter type 1:
741 molecular and pharmacological characterization of novel isoform variants and
742 chromosomal localization of the gene in the human and mouse genomes. Mol
743 Pharmacol 45:608–617.
744 38. Nishimura M, Tanaka S, Ihara F, Muroi Y, Yamagishi J, Furuoka H, Suzuki Y,
745 Nishikawa Y. 2015. Transcriptome and histopathological changes in mouse brain
746 infected with Neospora caninum. Sci Rep 5:7936.
747 39. Gomeza J, Ohno K, Hülsmann S, Armsen W, Eulenburg V, Richter DW,
748 Laube B, Betz H. 2003. Deletion of the mouse glycine transporter 2 results in a
749 hyperekplexia phenotype and postnatal lethality. Neuron 40:797–806.
750 40. Motokura T, Bloom T, Kim HG, Jüppner H, Ruderman JV, Kronenberg HM,
751 Arnold A. 1991. A novel cyclin encoded by a bcl1-linked candidate oncogene.
752 Nature 350:512–515.
753 41. Hopfner R, Mousli M, Jeltsch JM, Voulgaris A, Lutz Y, Marin C, Bellocq JP,
754 Oudet P, Bronner C. 2000. ICBP90, a novel human CCAAT binding protein,
755 involved in the regulation of topoisomerase IIalpha expression. Cancer Res
756 60:121–128.

757 42. Brodie C, Steinhart R, Kazimirsky G, Rubinfeld H, Hyman T, Ayres JN, Hur
758 GM, Toth A, Yang D, Garfield SH, Stone JC, Blumberg PM. 2004. PKCdelta
759 associates with and is involved in the phosphorylation of RasGRP3 in response to
760 phorbol esters. Mol Pharmacol 66:76–84.
761 43. Franco M, Shastri AJ, Boothroyd JC. 2014. Infection by Toxoplasma gondii
762 specifically induces host c-Myc and the genes this pivotal transcription factor
763 regulates. Eukaryotic Cell 13:483–493.
764 44. Dang CV, Lewis BC. 1997. Role of Oncogenic Transcription Factor c-Myc in
765 Cell Cycle Regulation, Apoptosis and Metabolism. J Biomed Sci 4:269–278.
766 45. Hill MM, Bastiani M, Luetterforst R, Kirkham M, Kirkham A, Nixon SJ,
767 Walser P, Abankwa D, Oorschot VMJ, Martin S, Hancock JF, Parton RG. 2008.
768 PTRF-Cavin, a conserved cytoplasmic protein required for caveola formation and
769 function. Cell 132:113–124.
770 46. Anderson RG. 1998. The caveolae membrane system. Annu Rev Biochem
771 67:199–225.
772 47. Wenz HM, Hinck L, Cannon P, Navre M, Ringold GM. 1992. Reduced
773 expression of AP27 protein, the product of a growth factor-repressible gene, is
774 associated with diminished adipocyte differentiation. Proc Natl Acad Sci USA
775 89:1065–1069.
776 48. Nishikawa Y. 2017. Towards a preventive strategy for neosporosis: challenges
777 and future perspectives for vaccine development against infection with Neospora
778 caninum. J Vet Med Sci 79:1374–1380.
779 49. Takeuchi O, Hoshino K, Akira S. 2000. Cutting edge: TLR2-deficient and
780 MyD88-deficient mice are highly susceptible to Staphylococcus aureus infection. J
781 Immunol 165:5392–5396.

782 50. Sibley LD, Messina M, Niesman IR. 1994. Stable DNA transformation in the
783 obligate intracellular parasite Toxoplasma gondii by complementation of
784 tryptophan auxotrophy. Proc Natl Acad Sci USA 91:5508–5512.
785 51. Tanaka S, Nishimura M, Ihara F, Yamagishi J, Suzuki Y, Nishikawa Y. 2013.
786 Transcriptome analysis of mouse brain infected with Toxoplasma gondii. Infection
787 and immunity 81:3609–3619.
788 52. Umeda K, Tanaka S, Ihara F, Yamagishi J, Suzuki Y, Nishikawa Y. 2017.
789 Transcriptional profiling of Toll-like receptor 2-deficient primary murine brain
790 cells during Toxoplasma gondii infection. PLOS ONE 12:e0187703.
791 53. Kanehisa M, Sato Y, Kawashima M, Furumichi M, Tanabe M. 2016. KEGG
792 as a reference resource for gene and protein annotation. Nucleic Acids Res
793 44:D457-462.
794 54. Yu G, Wang L-G, Han Y, He Q-Y. 2012. clusterProfiler: an R package for
795 comparing biological themes among gene clusters. OMICS 16:284–287.
796 55. Warnes GR, Bolker B, Bonebakker L, Gentleman R, Huber W, Liaw A,
797 Lumley T, Maechler M, Magnusson A, Moeller S. 2009. gplots: Various R
798 programming tools for plotting data.
799 56. Xie F, Sun G, Stiller JW, Zhang B. 2011. Genome-wide functional analysis of
800 the cotton transcriptome by creating an integrated EST database. PLoS ONE
801 6:e26980.
802
803

804 **FIGURE LEGENDS**

805 **FIG 1** Immunostimulatory effects of *Neospora* genes. (A) 293T cells were transfected
806 with the luciferase reporter plasmids and the expression vector of one of the 18
807 *Neospora* genes encoding dense granule proteins, *NcCYP*, or *NcPF*. Luciferase
808 activity is expressed as the fold increase over the background level in lysates prepared
809 from mock-transfected cells. (B) 293T cells were transfected with the luciferase
810 reporter plasmids and the expression vector for *Neospora* gene *NcGRA6*, *NcGRA7*,
811 *NcGRA14*, or *NcCYP*. Error bars represent the means ± standard deviations of
812 triplicate readings. The results represent two independent experiments with similar
813 results.

814

815 **FIG 2** Generation of *NcGRA6*-, *NcGRA7*-, *NcGRA14*-, and *NcCYP*-deficient parasites
816 and their phenotypes. (A) Western blots of the parental strain Nc1 and the *NcGRA6*-,
817 *NcGRA7*-, *NcGRA14*-, and *NcCYP*-deficient parasites. Anti-NcGRA6 mouse serum
818 detected a 33-kDa protein in the Nc1 strain, but not in the *NcGRA6*-deficient parasite
819 (KO). (*) Anti-NcGRA6 mouse serum detected nonspecific bands in the Nc1 strain
820 and the *NcGRA6*-deficient parasite. A rabbit anti-NcGRA7 antibody detected three
821 major proteins of 33, 26, and 18 kDa in the Nc1 strain, but not in the *NcGRA7*-
822 deficient (KO) parasite. Three major proteins of 39, 34, and 25 kDa were detected in
823 the *NcGRA7*-complemented parasite (Comp). Anti-NcGRA14 mouse serum detected
824 a 51-kDa protein in the Nc1 strain, but not in the N*cGRA14*-deficient (KO) parasite. A
825 rabbit anti-NcCYP antibody detected a 15-kDa protein in the Nc1 strain, but not in the
826 *NcCYP*-deficient (KO) parasite. NcSRS2 was used as the loading control. (B)
827 Infection rates of the different parasite lines in Vero cells at 24 h postinfection. (C)
828 Intracellular replication assay of the parasite lines in Vero cells at 48 h postinfection.

(D) Egress rates of the different parasite lines in Vero cells at 72 h postinfection. Each bar represents ta mean ± standard deviation (n = 4 for all groups), and the results represent two independent experiments with similar results. *Statistically significant differences relative to the value for Nc1, according to one-way ANOVA (B, D) or two-way ANOVA (C) and a Tukey–Kramer post hoc analysis ($P < 0.05$). Further details on the production of antisera, polyclonal antibodies, and monoclonal antibodies against the *N. caninum* proteins, the western blotting analysis, infection rate and growth of *N. caninum* lines, can be found in the Supplemental Methods in the Supplemental Material.

FIG 3 Parasite virulence in mice. Mice were infected with a lethal dose (1×10^6) of *N. caninum* tachyzoites of the parental strain Nc1, the deficient line (KO), and the *NcGRA7*-complemented parasite (Comp). The survival rates (surviving mice/total mice) were calculated for 60 days after infection. (A) Survival rates of the BALB/c mice (n = 6 per group) were Nc1: 2/6, 33.3%; *NcGRA6*KO: 2/6, 33.3%; *NcGRA7*KO: 5/6, 83.3%; *NcGRA14*KO: 4/6, 66.7%; *NcCYP*KO: 1/6, 16.7%. (B) Survival rates of the C57BL/6 mice (n = 6 per group) were Nc1: 1/6, 16.7%; *NcGRA6*KO: 3/6, 50.0%; *NcGRA7*KO: 6/6, 100%; *NcGRA14*KO: 1/6, 16.7%; *NcCYP*KO: 1/6, 16.7%. (C) Survival rates of the *Tlr2*$^{-/-}$ mice (n = 6 per group) were Nc1: 1/6, 16.7%; *NcGRA7*KO: 5/6, 83.3%. (D) Survival rates of the BALB/c mice (n = 8 per group) were Nc1: 1/8, 12.5%; *NcGRA7*KO: 5/8, 62.5%; *NcGRA7*-complemented: 2/8, 25.9%. The significance of the differences in survival at 60 days postinfection was analyzed with a χ^2 test (*$P < 0.05$).

FIG 4 RNA-seq analysis of macrophages infected with Nc1, *NcGRA7*-deficient parasite (KO), or *NcGRA7*-complemented parasite (Comp), and uninfected cells (NoI) (n = 3 per group). Further details on macrophage preparation can be found in the Supplemental Methods in the Supplemental Material. These data show the differential expression of genes associated with the presence or absence of NcGRA7. (A) Expression of all genes in the pathway "cytokine–cytokine receptor interaction" was plotted as a heatmap. (B) A cluster in panel A, which was upregulated when NcGRA7 expression was restored, is enlarged. Detailed expression data for the genes are shown in Table S3. (C) Principal components analysis was performed to gain an overview all the expression data and identify classification patterns.

FIG 5 Expression of the 20 most differentially expressed genes downregulated (A) or upregulated (B) in macrophages infected with Nc1, *NcGRA7*-deficient parasites (KO), or *NcGRA7*-complemented parasites (Comp) and uninfected cells (Mock). Bars represent mean counts per million (CPM) in triplicate samples, and error bars represent the standard deviation of each value. Detailed expression data for the genes are shown in Table S4.

FIG 6 Cytokine production in macrophages infected with Nc1, *NcGRA7*-deficient parasites (KO), or *NcGRA7*-complemented parasites (Comp) and uninfected cells (mock) at 20 h postinfection. Further details on macrophage preparation can be found in the Supplemental Methods in the Supplemental Material. IL-12p40 (A) and IL-6 (B) in the culture supernatant were analyzed with ELISAs. Each value represents the mean ± standard deviation of four replicate samples. Different letters above the bars in the graphs indicate statistically significant differences according to one-way

878 ANOVA and a Tukey–Kramer post hoc analysis ($P < 0.05$). The reproducibility of the
879 data was confirmed with two independent experiments.
880
881 **FIG 7** Expression of inflammatory markers, chemokines, and chemokine receptors in
882 BALB/c mice at 5 days postinfection with Nc1, *NcGRA7*-deficient parasite (KO), or
883 *NcGRA7*-complemented parasite (Comp) and in uninfected control mice. (A) Levels
884 of IFN-γ in ascites fluid. mRNA levels in peritoneal cells (B) and spleen (C) were
885 normalized to *Actb* mRNA levels. The values per individual (symbols) and mean
886 levels (horizontal lines) from two pooled independent experiments ($n = 3 + 4$) are
887 shown. *Statistically significant differences observed with one-way ANOVA and a
888 Tukey–Kramer post hoc analysis ($P < 0.05$).
889
890 **FIG 8** Parasite burdens in tissues of BALB/c mice at 12 days (A) and 20 days (B)
891 postinfection with Nc1, *NcGRA7*-deficient parasite (KO), or *NcGRA7*-complemented
892 parasite (Comp). Values are the numbers of parasites in 50 ng of tissue DNA. The
893 number of parasites per individual (symbols) and the mean levels (horizontal lines)
894 are shown (12 days: $n = 6$ for all groups; 20 days: $n = 5$ for Nc1; $n = 8$ for KO; $n = 6$
895 for Comp). Individuals with undetectable expression are not shown. *Statistically
896 significant differences detected with one-way ANOVA and a Tukey–Kramer post hoc
897 analysis ($P < 0.05$).
898
899 **FIG 9** Immunohistochemical analysis of brain tissues of mice 30 days after infection
900 with Nc1. Serial sections (A–B and C–D) of *N. caninum*-infected mouse brains were
901 analyzed. (A) Hematoxylin and eosin (HE) staining showing inflammatory and
902 necrotic lesions. (B) Immunohistochemical analysis with an anti-NcGRA7 antibody.

903 NcGRA7 signal was observed around the necrotic area. (C, D) Immunohistochemical
904 analysis with antibodies directed against NcGRA7 and *N. caninum*. Further details of
905 this pathological analysis can be found in the Supplemental Methods in the
906 Supplemental Material.

A

	CRE	NFAT	NFKB	SRF	MMTV-LTR
NcGRA1	0.99	0.86	0.87	0.57	0.89
NcGRA2	1.35	1.20	1.16	0.71	1.00
NcGRA3	0.91	0.93	0.84	0.60	1.01
NcGRA4	1.02	1.09	0.94	0.82	0.95
NcGRA5	1.22	1.18	1.21	0.89	1.50
NcGRA6	5.45	7.24	17.70	0.86	1.51
NcGRA7	1.49	4.17	1.25	1.15	1.06
NcGRA8	0.73	1.08	1.30	0.72	1.52
NcGRA9	1.19	1.37	1.29	1.25	1.03
NcGRA10	1.18	1.19	1.28	1.20	0.89
NcGRA12	1.08	1.59	1.11	1.11	1.67
NcGRA14	11.15	7.48	0.89	0.74	1.51
NcGRA16	1.19	1.00	1.22	1.31	1.13
NcGRA17	1.45	2.40	1.04	1.99	0.67
NcGRA21	1.53	1.50	1.30	1.12	0.73
NcGRA22	1.24	1.35	1.04	1.28	0.71
NcGRA23	1.24	1.23	1.08	0.96	0.69
NcGRA25	1.46	2.75	1.04	0.86	0.81
NcCyp	1.18	1.09	1.23	0.92	0.98
NcPF	1.16	1.09	1.23	0.92	0.98

B

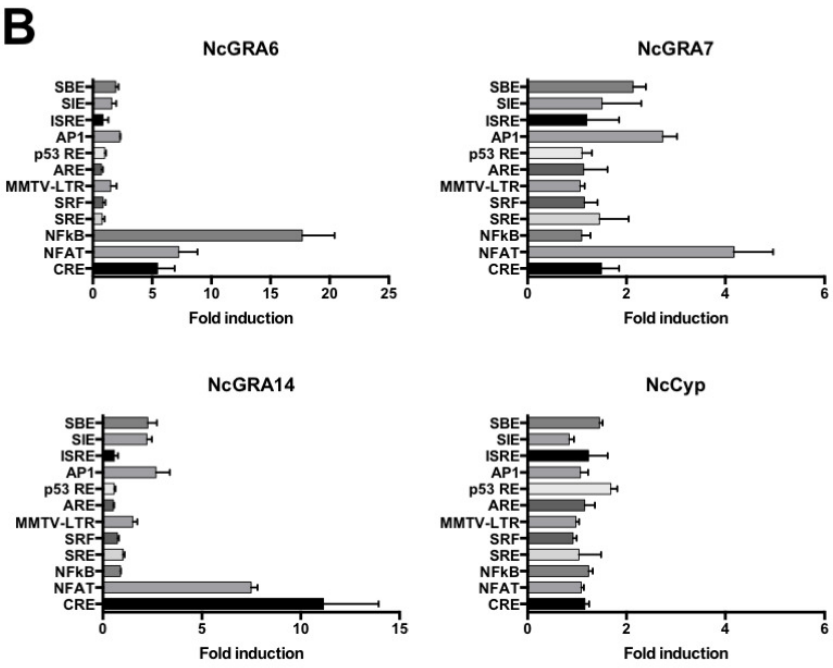

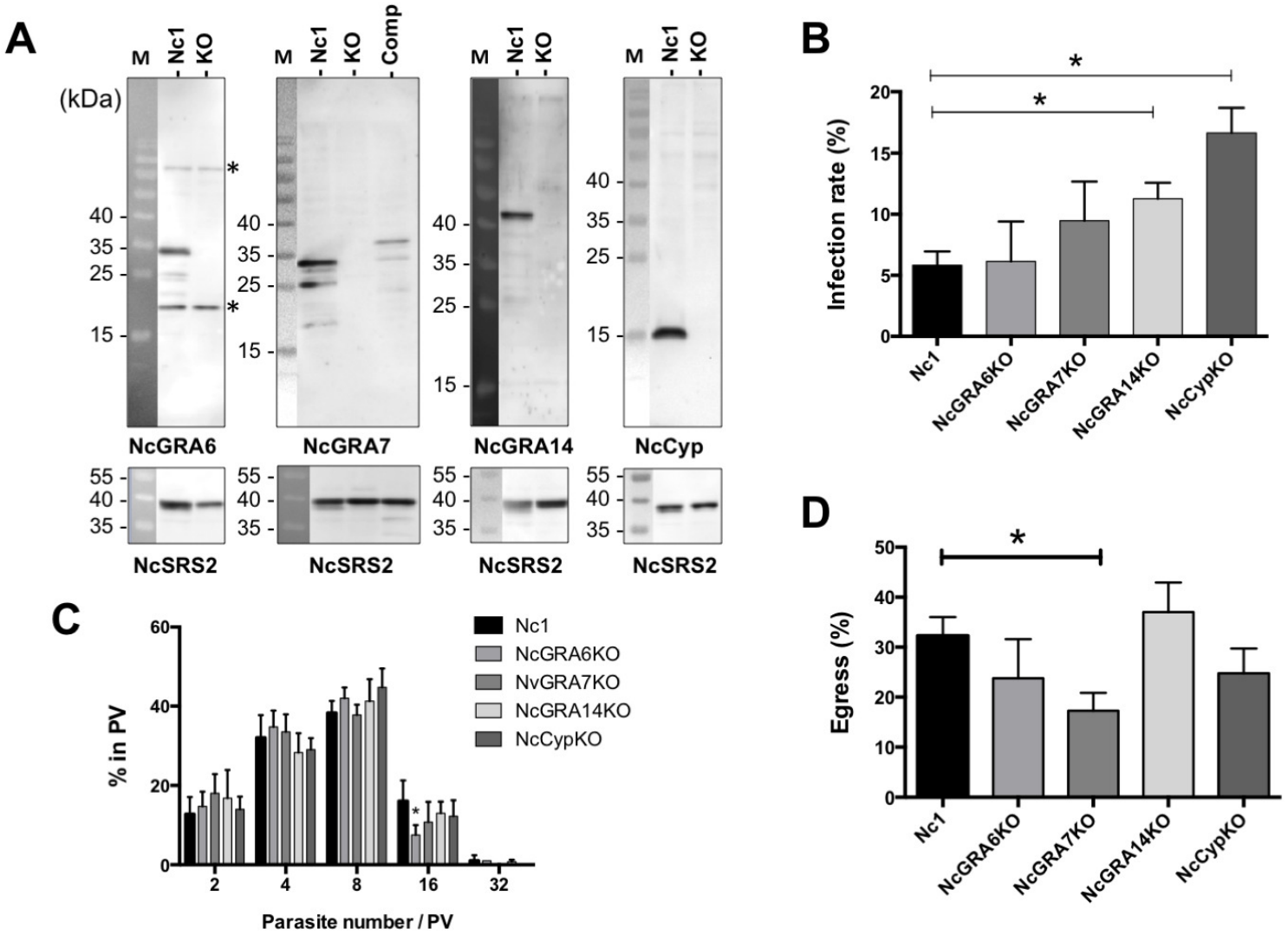
A
M
Nc1
KO
Comp
(kDa)
40
35
25
15
NcGRA6
NcGRA7
NcGRA14
NcCyp
55
40
35
NcSRS2
B
Infection rate (%)
20
15
10
5
0
Nc1
NcGRA6KO
NcGRA7KO
NcGRA14KO
NcCypKO
C
% in PV
60
40
20
0
2
4
8
16
32
Parasite number / PV
Nc1
NcGRA6KO
NvGRA7KO
NcGRA14KO
NcCypKO
D
Egress (%)
50
40
30
20
10
0

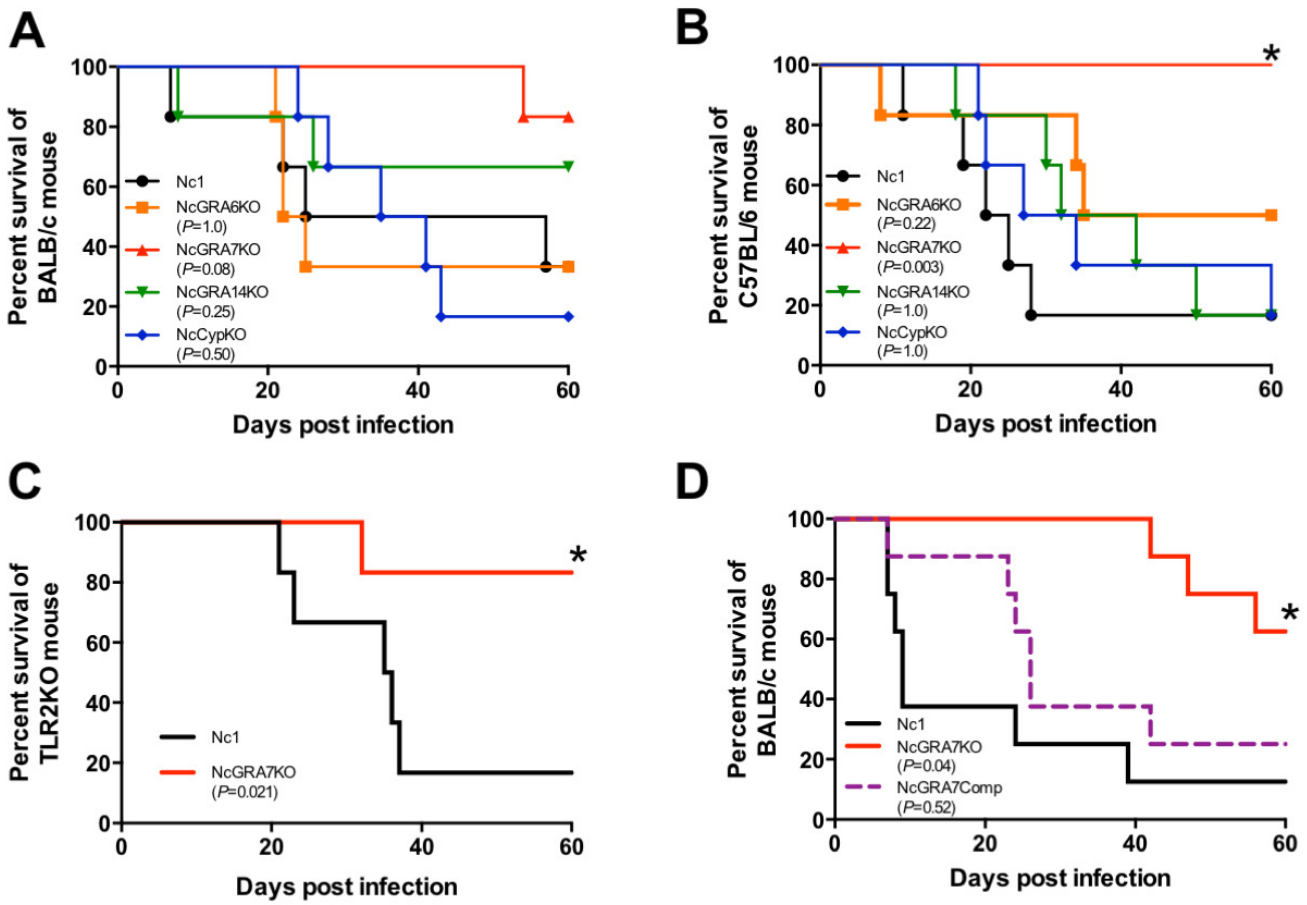
A
Percent survival of BALB/c mouse
Days post infection
Nc1
NcGRA6KO (P=1.0)
NcGRA7KO (P=0.08)
NcGRA14KO (P=0.25)
NcCypKO (P=0.50)
B
Percent survival of C57BL/6 mouse
Days post infection
Nc1
NcGRA6KO (P=0.22)
NcGRA7KO (P=0.003)
NcGRA14KO (P=1.0)
NcCypKO (P=1.0)
*
C
Percent survival of TLR2KO mouse
Days post infection
Nc1
NcGRA7KO (P=0.021)
*
D
Percent survival of BALB/c mouse
Days post infection
Nc1
NcGRA7KO (P=0.04)
NcGRA7Comp (P=0.52)
*

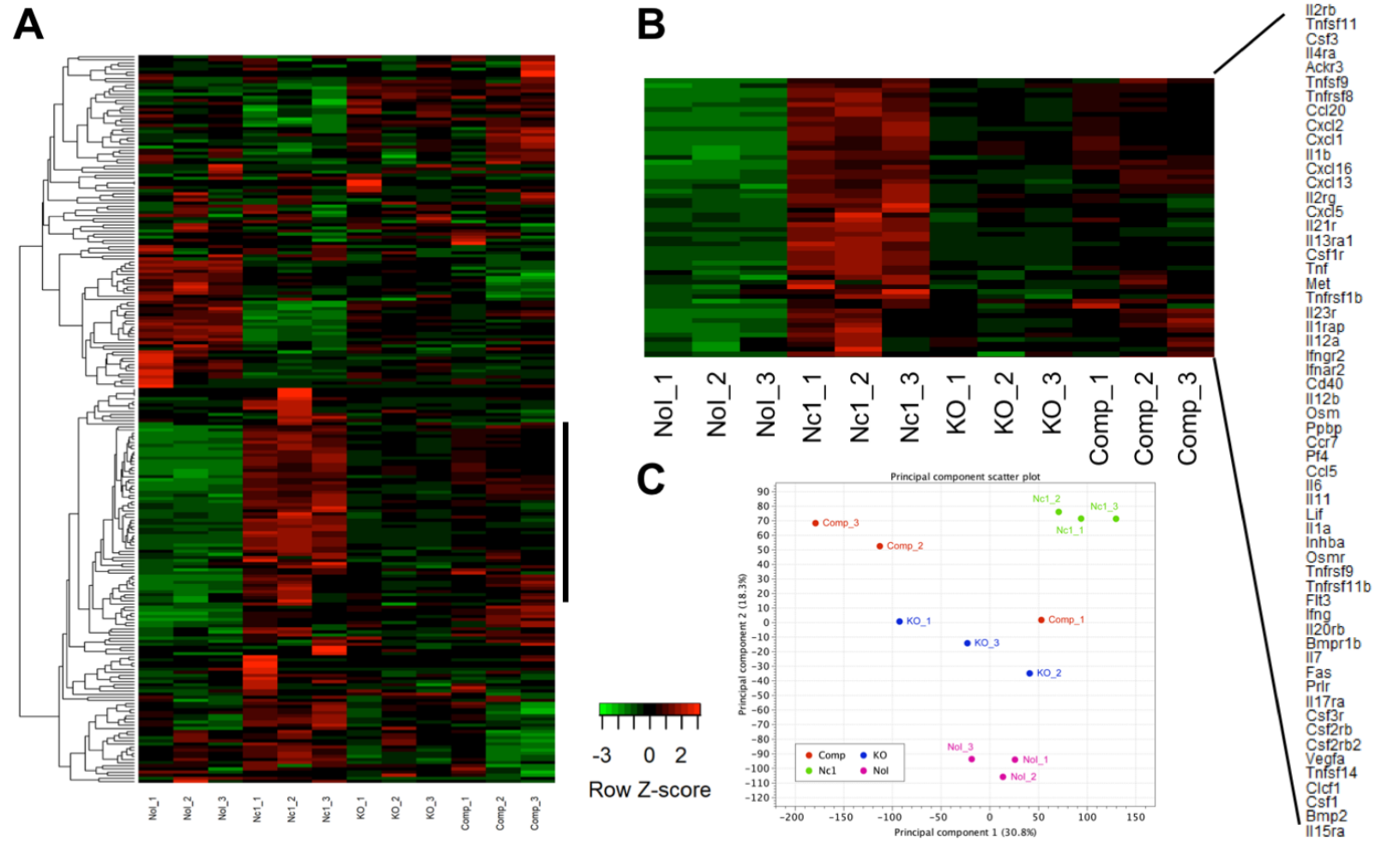
A
Nol_1
Nol_2
Nol_3
Nc1_1
Nc1_2
Nc1_3
KO_1
KO_2
KO_3
Comp_1
Comp_2
Comp_3
-3
0
2
Row Z-score
B
Nol_1
Nol_2
Nol_3
Nc1_1
Nc1_2
Nc1_3
KO_1
KO_2
KO_3
Comp_1
Comp_2
Comp_3
Il2rb
Tnfsf11
Csf3
Il4ra
Ackr3
Tnfsf9
Tnfrsf8
Ccl20
Cxcl2
Cxcl1
Il1b
Cxcl16
Cxcl13
Il2rg
Cxcl5
Il21r
Il13ra1
Csf1r
Tnf
Met
Tnfrsf1b
Il23r
Il1rap
Il12a
Ifngr2
Ifnar2
Cd40
Il12b
Osm
Ppbp
Ccr7
Pf4
Ccl5
Il6
Il11
Lif
Il1a
Inhba
Osmr
Tnfrsf9
Tnfrsf11b
Flt3
Ifng
Il20rb
Bmpr1b
Il7
Fas
Prlr
Il17ra
Csf3r
Csf2rb
Csf2rb2
Vegfa
Tnfsf14
Clcf1
Csf1
Bmp2
Il15ra
C
Principal component scatter plot
Principal component 2 (18.3%)
Principal component 1 (30.8%)
Comp_3
Comp_2
Nc1_2
Nc1_3
Nc1_1
KO_1
KO_3
KO_2
Comp_1
Nol_3
Nol_1
Nol_2
Comp
KO
Nc1
Nol

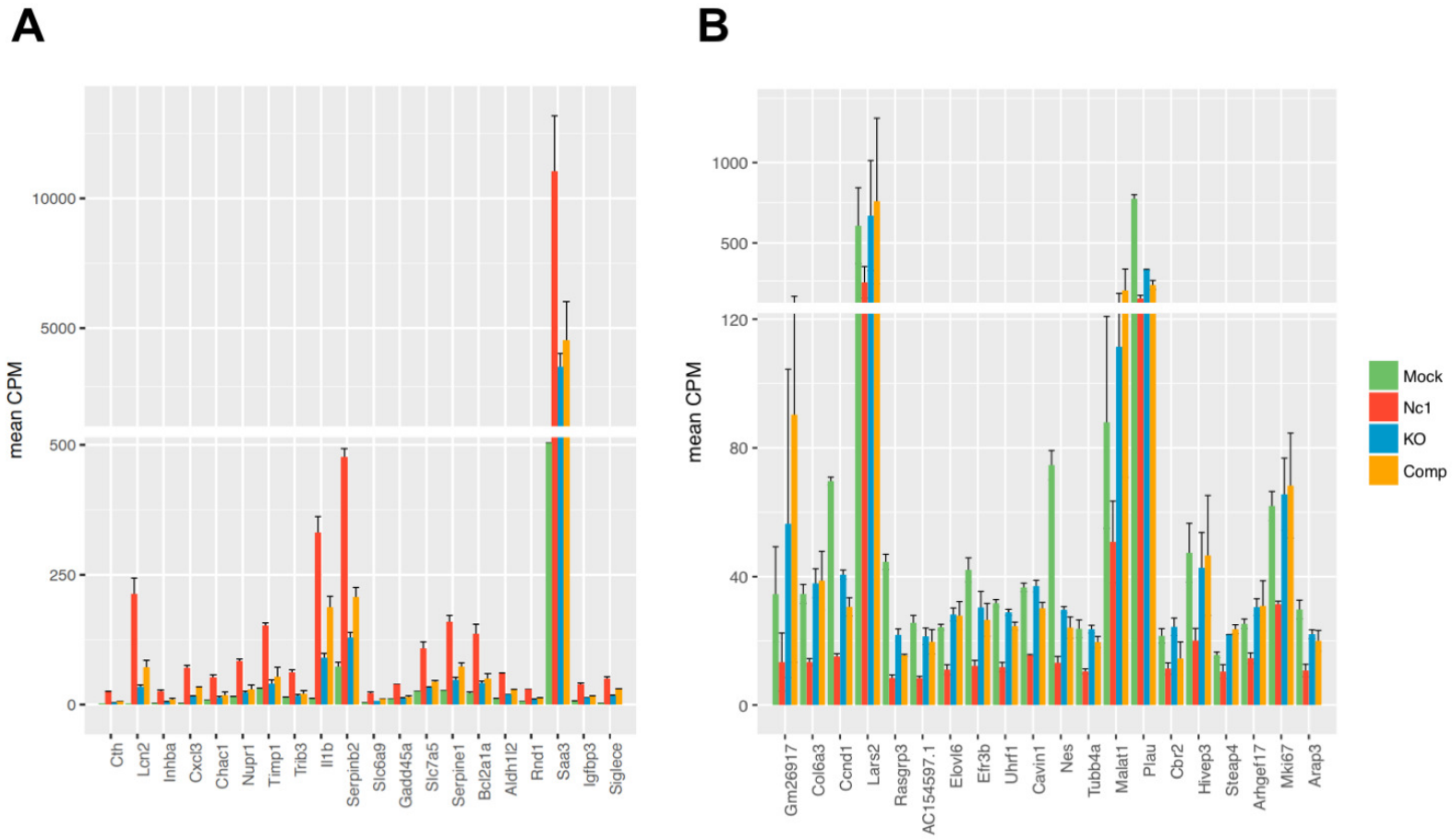
A
B
mean CPM
10000
5000
500
250
0
1000
500
120
80
40
0
Cth
Lcn2
Inhba
Cxcl3
Chac1
Nupr1
Timp1
Trib3
Il1b
Serpinb2
Slc6a9
Gadd45a
Slc7a5
Serpine1
Bcl2a1a
Aldh1l2
Rnd1
Saa3
Igfbp3
Siglece
Gm26917
Col6a3
Ccnd1
Lars2
Rasgrp3
AC154597.1
Elovl6
Efr3b
Uhrf1
Cavin1
Nes
Tubb4a
Malat1
Plau
Cbr2
Hivep3
Steap4
Arhgef17
Mki67
Arap3
Mock
Nc1
KO
Comp

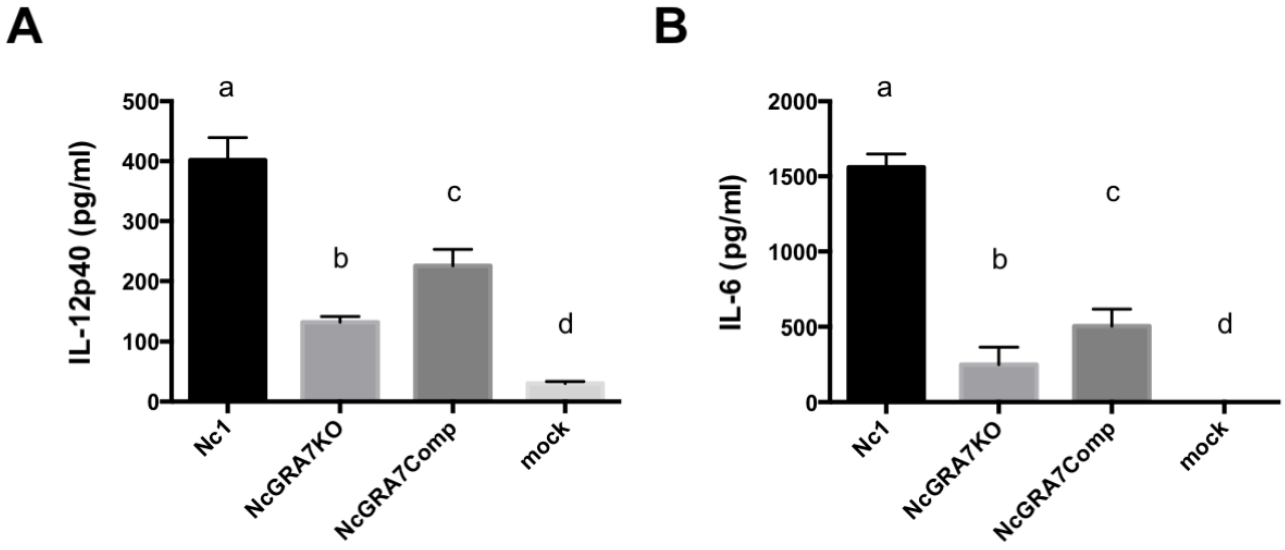
A
IL-12p40 (pg/ml)
500
400
300
200
100
0
a
b
c
d
Nc1
NcGRA7KO
NcGRA7Comp
mock
B
IL-6 (pg/ml)
2000
1500
1000
500
0
a
b
c
d
Nc1
NcGRA7KO
NcGRA7Comp
mock

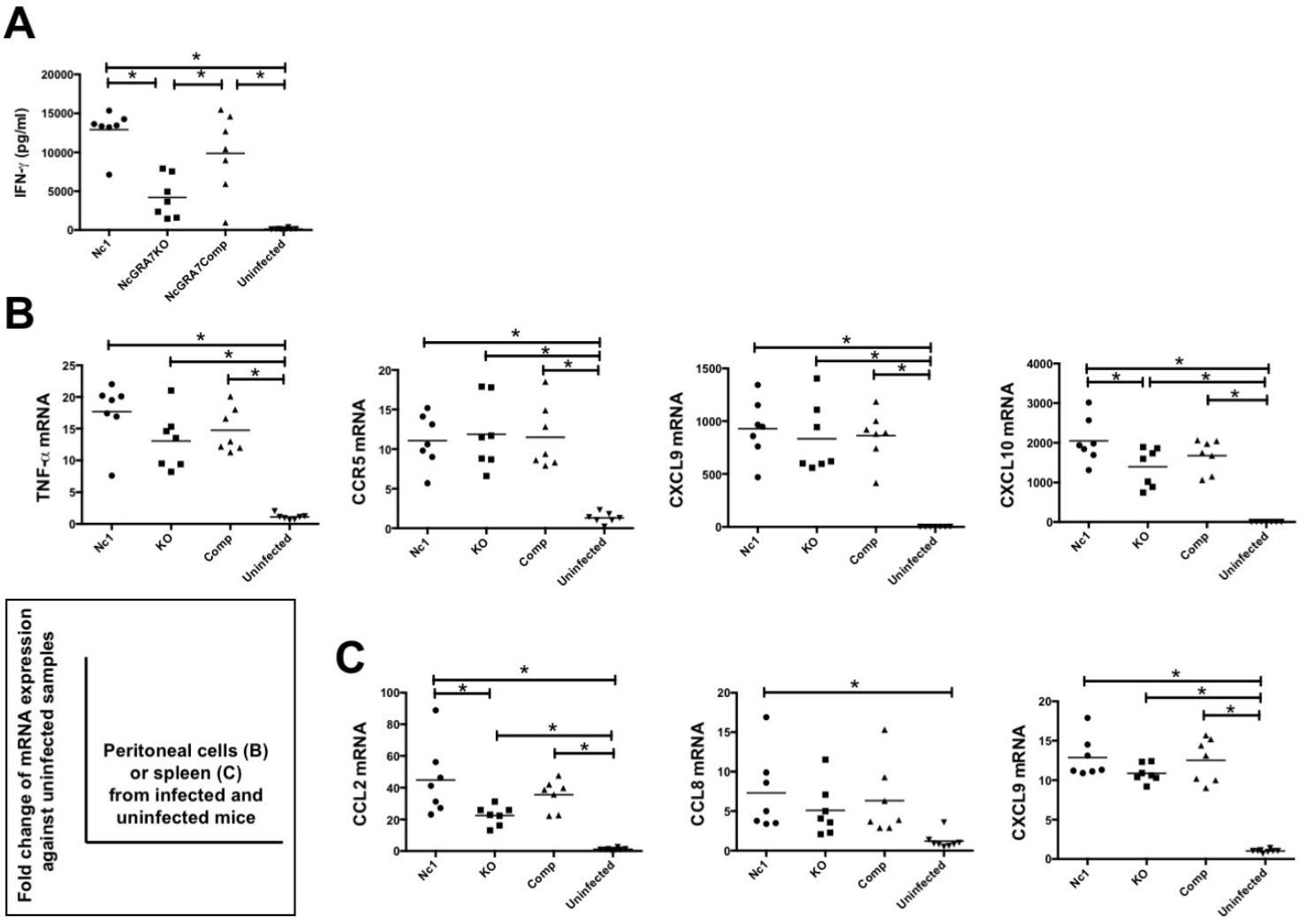
A
IFN-γ (pg/ml)
20000
15000
10000
5000
0
Nc1
NcGRA7KO
NcGRA7Comp
Uninfected
B
TNF-α mRNA
CCR5 mRNA
CXCL9 mRNA
CXCL10 mRNA
Nc1
KO
Comp
Uninfected
Fold change of mRNA expression against uninfected samples
Peritoneal cells (B) or spleen (C) from infected and uninfected mice
C
CCL2 mRNA
CCL8 mRNA
CXCL9 mRNA

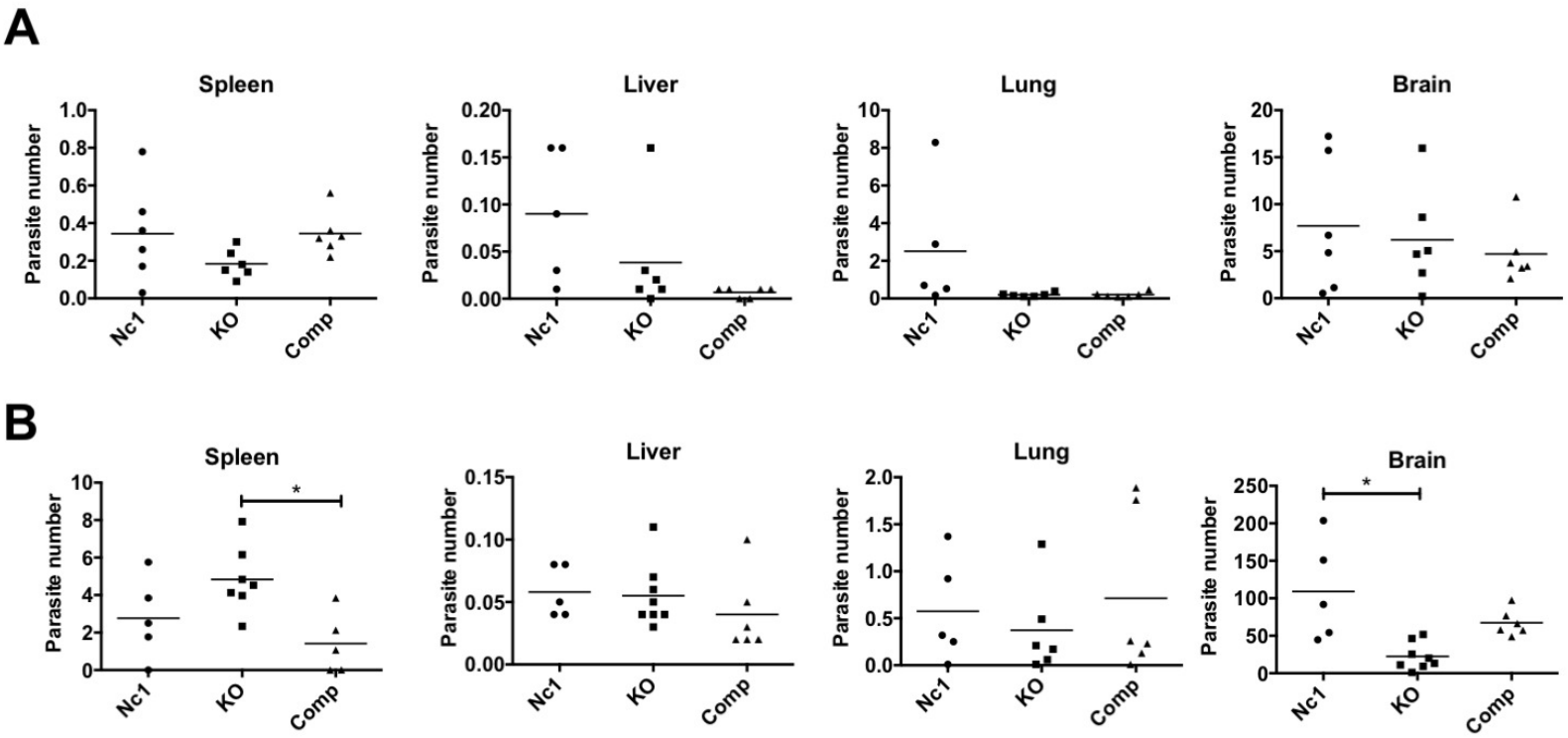
A
Spleen
Liver
Lung
Brain
Parasite number
Nc1
KO
Comp
B
Spleen
Liver
Lung
Brain
*
*

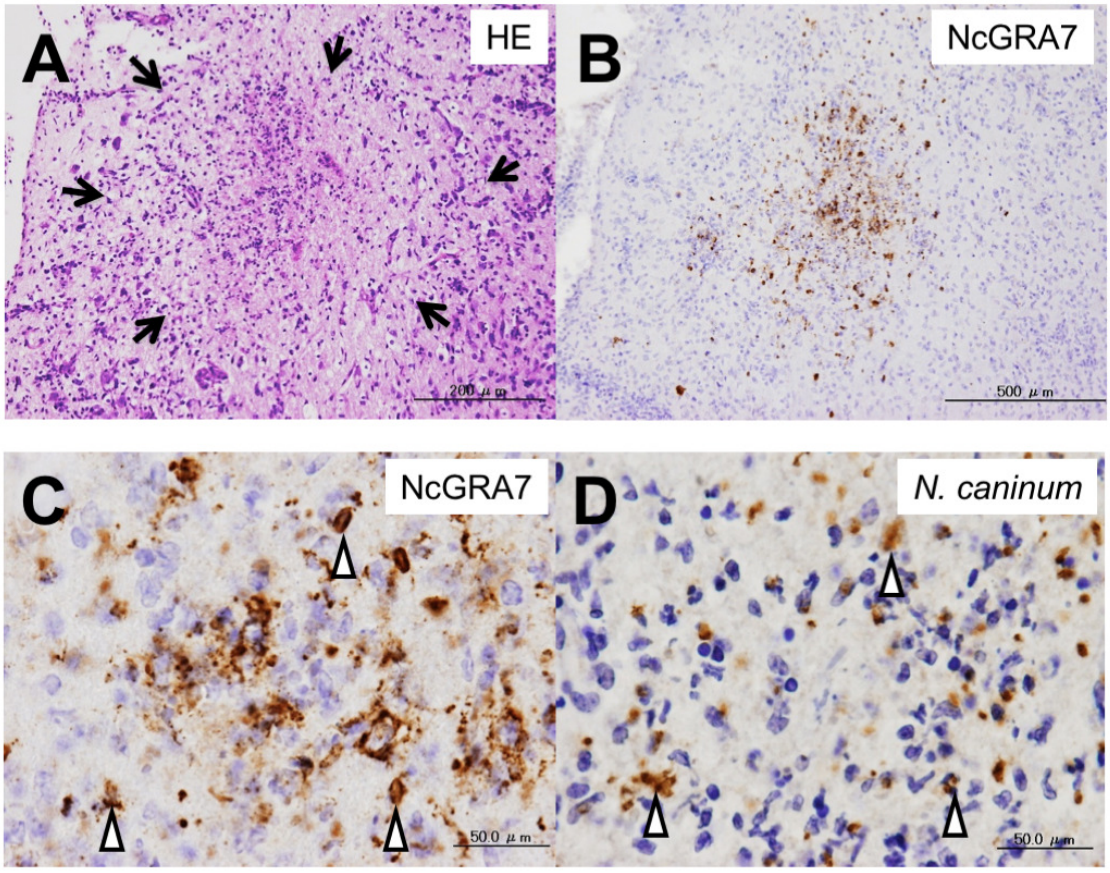
A
HE
200 μm
B
NcGRA7
500 μm
C
NcGRA7
50.0 μm
D
N. caninum
50.0 μm

Table 1. Plasmids used in this study

Plasmid	Description	Used for	reference
pSAG1::CAS9-U6::sgUPRT	CAS9 expressed from the *Toxoplasma* SAG1 promoter and CRISPR gRNA targeting *Toxoplasma* UPRT produced from the U6 promoter	CRISPR plasmid targeting *Toxoplasma* UPRT	Addgene
pSAG1::CAS9-U6::sgNcGRA6	CAS9 expressed from the *Toxoplasma* SAG1 promoter and CRISPR gRNA targeting NcGRA6 produced from the U6 promoter	CRISPR plasmid targeting between 86 b and 87 b in NcGRA6 gene	This study
pSAG1::CAS9-U6::sgNcGRA7	CAS9 expressed from the *Toxoplasma* SAG1 promoter and CRISPR gRNA targeting NcGRA7 produced from the U6 promoter	CRISPR plasmid targeting between 113 b and 114 b in NcGRA7 gene	This study
pSAG1::CAS9-U6::sgNcGRA14	CAS9 expressed from the *Toxoplasma* SAG1 promoter and CRISPR gRNA targeting NcGRA14 produced from the U6 promoter	CRISPR plasmid targeting between 110 b and 111 b in NcGRA14 gene	This study
pSAG1::CAS9-U6::sgNcCyp	CAS9 expressed from the *Toxoplasma* SAG1 promoter and CRISPR gRNA	CRISPR plasmid targeting between 753 b and 754 b in NcCyp gene	This study

	targeting NcCyp produced from the U6 promoter		
pUPRT::DHFR-D	DHFR* cassette flanked by two homology arms from the 5'- and 3'-UTR of UPRT gene respectively	Replacing the UPRT gene by DHFR*	Addgene
pSAG1::CAS9-U6::sgNcUPRT	CAS9 expressed from the *Toxoplasma* SAG1 promoter and CRISPR gRNA targeting *Neospora* UPRT produced from the U6 promoter	CRISPR plasmid targeting between 88 b and 89 b in *Neospora* UPRT	This study *Neospora* UPRT: NCLIV_056020
p3XFLAG-CMV-14		Plasmid for cloning of FLAG tag fused gene	Sigma-Aldrich
p3XFLAG-CMV-NcGRA1	FLAG tag-fused NcGRA1	Luciferase reporter assay	This study NCLIV_036400
p3XFLAG-CMV-NcGRA2	FLAG tag-fused NcGRA2	Luciferase reporter assay	This study NCLIV_045650
p3XFLAG-CMV-NcGRA3	FLAG tag-fused NcGRA3	Luciferase reporter assay	This study NCLIV_045870
p3XFLAG-CMV-NcGRA4	FLAG tag-fused NcGRA4	Luciferase reporter assay	This study NCLIV_054830
p3XFLAG-CMV-NcGRA5	FLAG tag-fused NcGRA5	Luciferase reporter assay	This study NCLIV_014150
p3XFLAG-CMV-NcGRA6	FLAG tag-fused NcGRA6	Luciferase reporter assay	This study NCLIV_052880
p3XFLAG-CMV-NcGRA7	FLAG tag-fused NcGRA7	Luciferase reporter assay, Insertion of FLAG tag-fused NcGRA7 DNA into	This study NCLIV_021640

		pDXF	
p3XFLAG-CMV-NcGRA8	FLAG tag-fused NcGRA8	Luciferase reporter assay	This study NCLIV_008990
p3XFLAG-CMV-NcGRA9	FLAG tag-fused NcGRA9	Luciferase reporter assay	This study NCLIV_066630
p3XFLAG-CMV-NcGRA10	FLAG tag-fused NcGRA10	Luciferase reporter assay	This study NCLIV_037450
p3XFLAG-CMV-NcGRA12	FLAG tag-fused NcGRA12	Luciferase reporter assay	This study NCLIV_041120
p3XFLAG-CMV-NcGRA14	FLAG tag-fused NcGRA14	Luciferase reporter assay	This study NCLIV_016360
p3XFLAG-CMV-NcGRA16	FLAG tag-fused NcGRA16	Luciferase reporter assay	This study NCLIV_003340
p3XFLAG-CMV-NcGRA17	FLAG tag-fused NcGRA17	Luciferase reporter assay	This study NCLIV_005560
p3XFLAG-CMV-NcGRA21	FLAG tag-fused NcGRA21	Luciferase reporter assay	This study NCLIV_017230
p3XFLAG-CMV-NcGRA22	FLAG tag-fused NcGRA22	Luciferase reporter assay	This study NCLIV_052190
p3XFLAG-CMV-NcGRA23	FLAG tag-fused NcGRA23	Luciferase reporter assay	This study NCLIV_006780
p3XFLAG-CMV-NcGRA25	FLAG tag-fused NcGRA24	Luciferase reporter assay	This study NCLIV_042680
p3XFLAG-CMV-NcCyp	FLAG tag-fused NcCyp	Luciferase reporter assay	This study NCLIV_004790
p3XFLAG-CMV-NcPF	NcPF	Luciferase reporter assay	This study NCLIV_00610
pGL4.29	cyclic AMP response , CRE	Luciferase reporter assay for cAMP/PKA signal	Promega
pGL4.30	Nuclear factor of activated T-cells response element, NFAT	Luciferase reporter assay for calcium/calcineurin signal	Promega
pGL4.32	Nuclear factor kB	Luciferase reporter	Promega

	response element, NF-kB	assay for NF-kB signal	
pGL4.33	Serum response element, SRE	Luciferase reporter assay for MAP/ERK signal	Promega
pGL4.34	Serum response factor response element, SRF	Luciferase reporter assay for RhoA signal	Promega
pGL4.36	Murine mouse mammary virus long terminal repeat, MMTV-LTR	Luciferase reporter assay for nuclear receptor signal (androgen receptor, glucocorticoid receptor, etc)	Promega
pGL4.37	Antioxidant response element, ARE	Luciferase reporter assay for oxidative stress signal	Promega
pGL4.38	p53 response element, p53 RE	Luciferase reporter assay for p53 signal	Promega
pGL4.44	AP1 response element, AP1	Luciferase reporter assay for MAPK/JNK signal	Promega
pGL4.45	Interferon-stimulated response element. ISRE	Luciferase reporter assay for IFN-alpha signal	Promega
pGL4.47	sis-inducible element, SIE	Luciferase reporter assay for IL-6 signal	Promega
pGL4.48	SMAD binding element, SBE	Luciferase reporter assay for TGF-beta signal	Promega
pGL4.74	Control Renilla luciferase expression vector		Promega
pDMG	Foreign gene expressed from the *Toxoplasma* GRA1	Plasmid for cloning of FLAG tag fused gene	Nishikawa et al., 2003. Int J Parasitol

	5'UTR and GRA2 3' UTR		33:1525–1535.
pDMG-NcGRA7FLAG	FLAG tag-fused NcGRA7 expressed from the Toxoplasma GRA1 5'UTR and GRA2 3' UTR	Replacing the UPRT gene by FLAG tag-fused NcGRA7	This study
pGEX4T-1/NcGRA6	Cloned NcGRA6 gene (130-462 bp) into EcoRI and XhoI sites of pGEX4T-1 plasmid	Preparation of recombinant NcGRA6 fused with GST	This study
pGEX4T-1/NcGRA14	Cloned NcGRA14 gene (109-852 bp) into EcoRI and XhoI sites of pGEX4T-1 plasmid	Preparation of recombinant NcGRA14 fused with GST	This study

Table 2. Primers used in this study

Primers	Sequence (5' -> 3')	Used for
NcGRA1-InFu-1F	ACCAGTCGAC**TCTAGA**TG GTGCGTGTGAGCGCT	To clone full length of NcGRA1 gene into *Xba*I and *Bam*HI sites of p3XFLAG-CMV-14 plasmid by In-fusion cloning
NcGRA1-InFu-2R	AGTCAGCCCG**GGATC**TAT GTTGCCCTTGAAGAGC	
NcGRA2-InFu-1F	ACCAGTCGAC**TCTAGA**TG TTCACGGGGAAACGTT	To clone full length of NcGRA2 gene into *Xba*I and *Bam*HI sites of p3XFLAG-CMV-14 plasmid by In-fusion cloning
NcGRA2-InFu-2R	AGTCAGCCCG**GGATC**TAT TGACTTCAGCTTCTGGC	
NcGRA3-InFu-1F	ACCAGTCGAC**TCTAGA**TG CCTGGTAAACAGGTGC	To clone full length of NcGRA3 gene into *Xba*I and *Bam*HI sites of p3XFLAG-CMV-14 plasmid by In-fusion cloning
NcGRA3-InFu-2R	AGTCAGCCCG**GGATC**TAT TTCTTTCGTGCTTGCGA	
NcGRA4-InFu-1F	ACCAGTCGAC**TCTAGA**TG AAGGGTCTCTTCTTTCC	To clone full length of NcGRA4 gene into *Xba*I and *Bam*HI sites of p3XFLAG-CMV-14 plasmid by In-fusion cloning
NcGRA4-InFu-2R	AGTCAGCCCG**GGATC**TAT GGCGCATTGCTTTCAAC	
NcGRA5-InFu-1F	ACCAGTCGAC**TCTAGA**TG GCGTCTGTCAAACGC	To clone full length of NcGRA5 gene into *Xba*I and *Bam*HI sites of p3XFLAG-CMV-14 plasmid by In-fusion cloning
NcGRA5-InFu-2R	AGTCAGCCCG**GGATC**TCT CTTCCTCTCCTGCTTC	
NcGRA6-InFu-1F	ACCAGTCGAC**TCTAGA**TG GCGAACAATAGAACCC	To clone full length of NcGRA6 gene into *Xba*I and *Bam*HI sites of p3XFLAG-CMV-14 plasmid by In-fusion cloning
NcGRA6-InFu-2R	AGTCAGCCCG**GGATC**GTT TTTCCTCCCCGCCGT	
NcGRA7-InFu-1F	ACCAGTCGAC**TCTAGA**TG GCCCGACAAGCAACC	To clone full length of NcGRA7 gene into *Xba*I and *Bam*HI sites of p3XFLAG-CMV-14 plasmid by In-fusion cloning
NcGRA7-InFu-2R	AGTCAGCCCG**GGATC**TTT CGGTGTCTACTTCCTG	
NcGRA8-InFu-1F	ACCAGTCGAC**TCTAGA**TG GCTGCAGTGCGCGTG	To clone full length of NcGRA8 gene into *Xba*I and *Bam*HI sites of p3XFLAG-CMV-14 plasmid by In-fusion cloning
NcGRA8-InFu-2R	AGTCAGCCCG**GGATC**TAG CATCTCCATTAGCCTC	
NcGRA9-InFu-1F	ACCAGTCGAC**TCTAGA**TG	To clone full length of NcGRA9 gene into

	ATGAGGTCATTCAAGTC	*Xba*I and *Bam*HI sites of p3XFLAG-CMV-14 plasmid by In-fusion cloning
NcGRA9-InFu-2R	AGTCAGCCCG**GGATC**GTATTTCTCCGTTATGGTTC	
NcGRA10-InFu-1F	ACCAGTCGAC**TCTAGA**TGCTGCTCTACTACCGC	To clone full length of NcGRA10 gene into *Xba*I and *Bam*HI sites of p3XFLAG-CMV-14 plasmid by In-fusion cloning
NcGRA10-InFu-2R	AGTCAGCCCG**GGATC**TATCACATTCCCCGCTGC	
NcGRA12-InFu-1F	ACCAGTCGAC**TCTAGA**TGGAGGTTGTTGTGGCG	To clone full length of NcGRA12 gene into *Xba*I and *Bam*HI sites of p3XFLAG-CMV-14 plasmid by In-fusion cloning
NcGRA12-InFu-2R	AGTCAGCCCG**GGATC**TGCGGGGACCGGCGTTTG	
NcGRA14-InFu-1F	ACCAGTCGAC**TCTAGA**TGCAGGGCGCAACGGGG	To clone full length of NcGRA14 gene into *Xba*I and *Bam*HI sites of p3XFLAG-CMV-14 plasmid by In-fusion cloning
NcGRA14-InFu-2R	AGTCAGCCCG**GGATC**TGTAGACCGAGTTACCTGA	
NcGRA16-InFu-1F	ACCAGTCGAC**TCTAGA**TGTATCGGAGTCAATCGC	To clone full length of NcGRA16 gene into *Xba*I and *Bam*HI sites of p3XFLAG-CMV-14 plasmid by In-fusion cloning
NcGRA16-InFu-2R	AGTCAGCCCG**GGATC**TCTGAGTCCCATCTTCGTC	
NcGRA17-InFu-1F	ACCAGTCGAC**TCTAGA**TGCGAGTGTGCGGTTCC	To clone full length of NcGRA17 gene into *Xba*I and *Bam*HI sites of p3XFLAG-CMV-14 plasmid by In-fusion cloning
NcGRA17-InFu-2R	AGTCAGCCCG**GGATC**TCTGGTTGCCACTGCCGG	
NcGRA21-2-InFu-1F	ACCAGTCGAC**TCTAGA**TGATACATCAGCACCGATG	To clone full length of NcGRA21 gene into *Xba*I and *Bam*HI sites of p3XFLAG-CMV-14 plasmid by In-fusion cloning
NcGRA21-2-InFu-2R	AGTCAGCCCG**GGATC**TGAGAGAAACGCAACGTTG	
NcGRA22-InFu-1F	ACCAGTCGAC**TCTAGA**TGTGGATTTTGTTGTGTATG	To clone full length of NcGRA22 gene into *Xba*I and *Bam*HI sites of
NcGRA22-InFu-2	AGTCAGCCCG**GGATC**TAT	

R	TGCGCCCGTTCTTTAG	p3XFLAG-CMV-14 plasmid by In-fusion cloning
NcGRA23-InFu-1F	ACCAGTCGAC**TCTAGA**TGCTCGCGTCCGCCGAC	To clone full length of NcGRA23 gene into *Xba*I and *Bam*HI sites of p3XFLAG-CMV-14 plasmid by In-fusion cloning
NcGRA23-InFu-2R	AGTCAGCCCG**GGATC**TGTTCTTTCGCGCGAGCA	
NcGRA25-InFu-1F	ACCAGTCGAC**TCTAGA**TGAAACGGTCCTCAGTATG	To clone full length of NcGRA25 gene into *Xba*I and *Bam*HI sites of p3XFLAG-CMV-14 plasmid by In-fusion cloning
NcGRA25-InFu-2R	AGTCAGCCCG**GGATC**TACGACGAGTTTGTTGAAGA	
NcCyp-InFu-1F	ACCAGTCGAC**TCTAGA**TGAAGCTCCTGTTCTTCTT	To clone full length of NcCyp gene into *Xba*I and *Bam*HI sites of p3XFLAG-CMV-14 plasmid by In-fusion cloning
NcCyp-InFu-2R	AGTCAGCCCG**GGATC**TCAACAAACCAATGTCCGTG	
NcPF_EcoRI_1F	AC**GAATTC**ATGTCGGACTGGGATCCCGT	To clone full length of NcPF gene into *Eco*RI and *Xba*I sites of p3XFLAG-CMV-14 plasmid
NcPF_XbaI_2R	CC**TCTAGA**TTAATAGCCAGACTGGTGAA	
Common CAS9-U6-Rv	AACTTGACATCCCCATTTAC	Common primer for CRISPR/CAS9 plasmids targeting *Neospora* genes
NcGRA6_70-gRNAv2	GTGACGCTTGTGGCCTTCATGTTTTAGAGCTAGAAATAGC	Primer for CRISPR/CAS9 plasmids targeting NcGRA6 gene (pSAG1::CAS9-U6::sgNcGRA6)
NcGRA7_97-gRNAv2	GAACAGCATGAAGGGGACATGTTTTAGAGCTAGAAATAGC	Primer for CRISPR/CAS9 plasmids targeting NcGRA7 gene (pSAG1::CAS9-U6::sgNcGRA7)
NcGRA14_94-gRNAv2	GTTGTTTCAGCTGCTGGCTTGTTTTAGAGCTAGAAATAGC	Primer for CRISPR/CAS9 plasmids targeting NcGRA14 gene (pSAG1::CAS9-U6::sgNcGRA14)
NcCyp_169-gRNAv2	GGTCTCTTCGACAAGTACAAGTTTTAGAGCTAGAAATAGC	Primer for CRISPR/CAS9 plasmids targeting NcCyp gene (pSAG1::CAS9-U6::sgNcCyp)
NcUPRT_72 – gRNAv2	GCAGGAGGAAAGCATTCTGCGTTTTAGAGCTAGAAA	Primer for CRISPR/CAS9 plasmids targeting NcUPRT gene

	TAGC	(pSAG1::CAS9-U6::sgUPRT)
DHFR-25ntNcGRA6_70_1F	TGTTGGCGGTGACGCTTGTGGCCTTAAGCTTCGCCAGGCTGTAAA	To amplify an amplicon containing NcGRA6 homology regions surrounding a pyrimethamine-resistant DHFR* cassette
DHFR-21ntNcGRA6_70_2R	GAGCTGAGAGGCACGCCCATGGGAATTCATCCTGCAAGTGCATAG	
DHFR-NcGRA7_97_1F	TGGCAACCGAACAGCATGAAGGGGAAAGCTTCGCCAGGCTGTAAA	To amplify an amplicon containing NcGRA7 homology regions surrounding a pyrimethamine-resistant DHFR* cassette
DHFR-NcGRA7_97_2R	GCCCTAACCCCATATCCGATGGGAATTCATCCTGCAAGTGCATAG	
DHFR-25ntNcGRA14_94_1F	GTTCAACAGTTGTTTCAGCTGCTGGAAGCTTCGCCAGGCTGTAAA	To amplify an amplicon containing NcGRA14 homology regions surrounding a pyrimethamine-resistant DHFR* cassette
DHFR-21ntNcGRA14_94_2R	CGGTACGAAATCTCGCCCAAGGGAATTCATCCTGCAAGTGCATAG	
DHFR-NcCyp_169_1Fv2	ACTTCATTGGTCTCTTCGACAAGTAAAGCTTCGCCAGGCTGTAAA	To amplify an amplicon containing NcCyp homology regions surrounding a pyrimethamine-resistant DHFR* cassette
DHFR-NcCyp_169_2Rv2	CGGTGGAACGTGCTGCCTTTGGGAATTCATCCTGCAAGTGCATAG	
3xFLAG_pDXF_1F_rev	ATCAAGAAGCTTGATAAGCTTGCGGCCGCGAAT	To amplify NcGRA7-FLAG expressed from the Toxoplasma GRA1-5'UTR and GRA2-3' UTR
3xFLAG_pDXF_2R	CTGCAGGAATTCGATGGGATCACTACTTGTCATC	
NcGRA6-screen-1F	ATGGCGAACAATAGAACCCTC	To confirm the insertion of DHFR* cassette into NcGRA6 gene
NcGRA6-screen-2R	CCCACGGCGACTGGCGGCTCA	To confirm the insertion of DHFR* cassette into NcGRA6 gene
NcGRA7-screen-1F	ATGGCCCGACAAGCAACCTTC	To confirm the insertion of DHFR* cassette into NcGRA7 gene and NcGRA7-FLAG cassette into NcUPRT

		gene
NcGRA7-screen-2R	TACTGCCAGCTTCTTGATCAA	To confirm the insertion of DHFR* cassette into NcGRA7 gene and NcGRA7-FLAG cassette into NcUPRT gene
NcGRA14-screen-1F	ATGCAGGGCGCAACGGGGCGA	To confirm the insertion of DHFR* cassette into NcGRA14 gene
NcGRA14-screen-2R	ACTACCAAAACGTTCCACCGC	To confirm the insertion of DHFR* cassette into NcGRA14 gene
NcCyp-screen-1Fv2	GGCGACGTGGTCCCTAAGAC	To confirm the insertion of DHFR* cassette into NcCyp gene
NcCyp-screen-2R	CTCGTCTTCGAATCTGGGGCC	To confirm the insertion of DHFR* cassette into NcCyp gene
TgDHFR-TS-screen-2R	CAGACACACCGGTTTCTGCAT	To confirm the insertion of DHFR* cassette into target gene
DHFR2-1F	CCATTGTGAACATCCTCAAC	To confirm the insertion of DHFR* cassette into target gene
NcUPRT(-6-14)1F	TCTTTGATGGCACAGACACC	To confirm the insertion of NcGRA7-FLAG cassette into NcUPRT gene
NcUPRT(265-284)2R	AAAAGCACTGCACAACATGC	To confirm the insertion of NcGRA7-FLAG cassette into NcUPRT gene
rNcGRA6_1F_130	AT**GAATTC**ATGGATCCGGTTGAATCCGTGGAG	To clone NcGRA6 gene (130-462 bp) into *Eco*RI and *Xho*I sites of pGEX4T-1 plasmid
rNcGRA6_2R_462	AT**CTCGAG**CTATCTGTGACGTGCCTGCTGCCG	
rNcGRA14_1F_109	GC**GAATTC**ATGGGCTTGGGCGAGATTTCGTAC	To clone NcGRA14 gene (109-852 bp) into *Eco*RI and *Xho*I sites of pGEX4T-1 plasmid
rNcGRA14_2R_852	AT**CTCGAG**CTACCGAGACTTGCCTCCGGATGT	
TNFa-1F	GGCAGGTCTACTTTGGAGTCATTGC	Real-time PCR for expression of mouse TNF-alpha mRNA
TNFa-2R	ACATTCGAGGCTCCAGTGAA	
IFNg_1F	GAGGAACTGGCAAAAGG	Real-time PCR for expression of mouse

	ATG	IFN-gamma mRNA
IFNg_2R	TGAGCTCATTGAATGCTTGG	
NOS2_1F	CATTGGAAGTGAAGCGTTTCG	Real-time PCR for expression of mouse iNOS mRNA
NOS2_2R	CAGCTGGGCTGTACAAACCTT	
CCR5_1F	GACATCCGTTCCCCCTACAAG	Real-time PCR for expression of mouse CCR5 mRNA
CCR5_2R	TCACGCTCTTCAGCTTTTTGCAG	
CXCR6_1F	CCCTGTACTTTATGCCTTTG	Real-time PCR for expression of mouse CXCR6 mRNA
CXCR6_2R	CTTGGAACTGTCCTCAGAAG	
CCL2_1F	GGCTCAGCCAGATGCAGTTAA	Real-time PCR for expression of mouse CCL2 mRNA
CCL2_2R	CCTACTCATTGGGATCATCTTGCT	
CCL5-1F	CCAATCTTGCAGTCGTGTTTGT	Real-time PCR for expression of mouse CCL5 mRNA
CCL5-2R	CATCTCCAAATAGTTGATGTATTCTTGAAC	
CCL7_1F	GGATCTCTGCCACGCTTCTG	Real-time PCR for expression of mouse CCL7 mRNA
CCL7_2R	GGCCCACACTTGGATGCT	
CCL8_1F	CTGGGCCAGATAAGGCTCC	Real-time PCR for expression of mouse CCL8 mRNA
CCL8_2R	CATGGGGCACTGGATATTGT	
CCL17_1F	ATGTAGGCCGAGAGTGCTGC	Real-time PCR for expression of mouse CCL17 mRNA
CCL17_2R	TGATAGGAATGGCCCCTTTG	
CCL22_1F	TCGCTTTTCCTCTCTGAGC	Real-time PCR for expression of mouse

	C	CCL22 mRNA
CCL22_2F	GCCCTTTGTGGTCCCATATG	
CXCL9-1F	ACCTCAAACAGTTTGCCCCA	Real-time PCR for expression of mouse CXCL9 mRNA
CXCL9-2R	TTCACATTTGCCGAGTCCG	
CXCL10-1F	TGCCGTCATTTTCTGCCTCA	Real-time PCR for expression of mouse CXCL10 mRNA
CXCL10-2R	TCACTGGCCCGTCATCGATAT	
Nc5-1F	ACTGGAGGCACGCTGAACAC	Quantitative PCR for calculating parasite numbers based on the detection of *N. caninum* DNA
Nc5-2R	AACAATGCTTCGCAAGAGGAA	
Beta actin-1F	GCTCTGGCTCCTAGCACCAT	Internal control gene for real-time RT-PCR analysis
Beta actin-2R	GCCACCGATCCACACAGAGT	